Refrigerant Charge Loss Detection for a Mobile Air Conditioning System

C. E. Johnston, N. R. Miller and W. E. Dunn

ACRC TR-125 July 1997

For additional information:

Air Conditioning and Refrigeration Center
University of Illinois
Mechanical & Industrial Engineering Dept.
1206 West Green Street
Urbana, IL 61801

(217) 333-3115

Prepared as part of ACRC Project 78
Modeling, Diagnostics, and Control
for Mobile Air-Conditioning Systems
N. R. Miller and W. E. Dunn, Principal Investigators

The Air Conditioning and Refrigeration Center was founded in 1988 with a grant from the estate of Richard W. Kritzer, the founder of Peerless of America Inc. A State of Illinois Technology Challenge Grant helped build the laboratory facilities. The ACRC receives continuing support from the Richard W. Kritzer Endowment and the National Science Foundation. The following organizations have also become sponsors of the Center.

Amana Refrigeration, Inc.
Brazeway, Inc.
Carrier Corporation
Caterpillar, Inc.
Copeland Corporation
Dayton Thermal Products
Delphi Harrison Thermal Systems
Eaton Corporation
Ford Motor Company
Frigidaire Company
General Electric Company
Hydro Aluminum Adrian, Inc.
Indiana Tube Corporation
Lennox International, Inc.
Modine Manufacturing Co.
Peerless of America, Inc.
Redwood Microsystems, Inc.
The Trane Company
Whirlpool Corporation
York International, Inc.

For additional information:

Air Conditioning & Refrigeration Center
Mechanical & Industrial Engineering Dept.
University of Illinois
1206 West Green Street
Urbana IL 61801

217 333 3115

Table of Contents

Page

LIST OF TABLES

Page

LIST OF FIGURES

Page

1. INTRODUCTION.

1.1 Motivation

1.1.1 Environmental Concerns.

The release of toxic materials into the atmosphere has become a very important environmental issue over the past two decades. One of the chemical groups that has been targeted as bad for the environment is cloro-flourocarbons. Previous to 1992 automotive air conditioning systems used a refrigerant that fell into this category. Other refrigerants were developed and put into use, such as hydro-florocarbon R-134a that is commonly used today. While these new refrigerants are an improvement, they still have a negative impact when released into the environment. According to Amann [1], "the greenhouse effect of HFC-134a is estimated to be only about 10% that of CFC-12"; therefore, the improved refrigerant is still harmful. Detecting system charge loss early will reduce the amount of refrigerant being released into the environment.

1.1.2 Cost Savings.

It would also be advantageous to know when the air conditioning system is not working properly and what is causing the problem. As it is now, the driver's first indication that something is not right is when the air exiting the ducts is not cool. The mechanic has no indication of what the problem might be, and he must spend time performing tests to try to determine what is wrong with the system. The time that the mechanic spends searching for the problem costs money for the owner or automotive company. If the car could tell the mechanic what the problem is or at least narrow it down to a couple of options, time and money could be saved.

Often by the time the driver realizes that the air is not cool, serious damage has been done to the air conditioning compressor. In an automotive system, the oil that lubricates the compressor circulates in the system along with the refrigerant. The oil is pulled along by the high velocity of the refrigerant, but as the charge decreases, the velocity decreases as well. Some of the oil begins to collect inside some of the major components as well as the walls of the hoses; therefore, less oil circulates through the compressor to keep it lubricated. If the oil film on the compressor cylinder wall becomes too thin, wear begins to occur between the piston and cylinder wall. Over the past two

decades automotive companies have continued to increase the length of their warranties, and they are replacing more and more compressors at their expense. By 1990 approximately nine out of every ten new cars in the U.S. were air conditioned, and that number has surely gone up since then [2]. If the automotive manufacturers could cheaply and reliably detect charge loss, they could save a significant amount of money.

1.1.3 Customer Satisfaction.

A refrigerant charge loss detection system could also increase customer satisfaction. If the car alerts the user early enough that charge loss has occurred, the owner can schedule to get the problem repaired in a timely fashion before the system loses its cooling capacity. As it is now, the user does not know anything is wrong until he realizes that the system is no longer cooling the car cabin. At this point, the owner may have to go for several days or more without air conditioning. Repair times will often be shorter, and the car will be returned to the owner sooner.

1.2 Project Goal

The basic goal of this project is to develop a practical, on-line method for a vehicle to detect when a fault has occurred in the air conditioning system and alert the driver to the problem with some sort of warning device. The term practical means that the system must be very inexpensive and extremely reliable in order to implement it on a production vehicle. To keep the costs of the system down it was necessary to avoid expensive sensors such as pressure transducers and humidity measuring devices. The amount of computing power necessary to implement data acquisition, reduction, and analysis was kept in mind during the process because added computing power means added cost. The use of data already available on most vehicle buses was a high priority because this data is "free" in a sense.

The main focus of this study was refrigerant charge loss detection. This is a common problem, and for the reasons discussed in section 1.1 it is detrimental to the environment and the health of the compressor. Refrigerant charge loss cannot be avoided in the current systems being used. Leaks are commonly caused by damaged or missing O-ring seals at the various hose and component connections [2]. Even if there were no leaks at all at the connections and seals, refrigerant slowly seeps through the hoses

currently being used in the automotive industry [3]. Rigid lines, such as copper, could eliminate this problem, but the lines must be flexible to hold up under the flexing and vibrations that are inevitable in an automobile.

Other air conditioning system faults can occur, but refrigerant charge loss is the most common and concerning fault. Condenser fouling is also a common problem for air conditioning systems on off road vehicles and machinery. While this fault is normally not detrimental to the integrity of the system, it will affect the performance of the system. The possibility of a restricted condenser giving a false positive for charge loss could also arise. In other words, will a fouled condenser trigger the method used to detect refrigerant charge loss? If the system could tell the driver what the problem is, it could be fixed in a timely and least inexpensive method. This could avoid a costly repair such as the replacement of the air conditioning compressor.

1.3 Basic Air Conditioning System.

There are several types and variations of air conditioning systems; so, it is important that the reader knows the basic system that is discussed in this paper. The system has five main components: condenser, evaporator, expansion device, compressor, and accumulator. Figure 1.1 shows the basic schematic of an automotive air conditioning system.

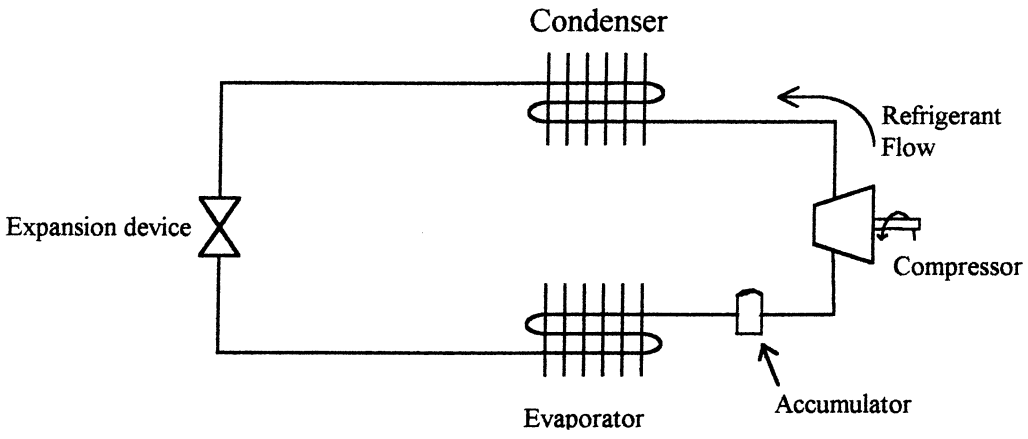

Figure 1.1 Basic Schematic of an Automotive A/C System.

For our system the expansion device is a simple fixed displacement orifice tube, but some systems use a thermal expansion valve (TXV). A TXV attempts to control a predetermined amount of refrigerant superheat at the outlet of the evaporator. This is accomplished by varying the size of the opening, and therefore pressure drop, of the TXV. The compressor in our system is also a fixed displacement design, but variable displacement compressors are also common. The amount of displacement is controlled by the suction line pressure. The orifice tube-fixed displacement compressor combination is found in many production vehicles, and all of the test results reported in this thesis were performed on such a system. The evaporator is an aluminum plate-fin design which is very common in newer vehicles, and the condenser is a tube-fin design. Most A/C systems have an accumulator on the low pressure side (or a receiver on the high pressure side). It is undesirable to have significant amounts of liquid refrigerant entering the compressor; therefore, the accumulator traps any liquid refrigerant exiting the evaporator. Since the accumulator is housed in the hot engine compartment, the trapped liquid refrigerant evaporates before entering the compressor.

1.4 A/C Fault Diagnosis

The most common air conditioning fault is the loss of refrigerant charge, and over time this problem is unavoidable. Currently, it is up to the driver to sense when the system is not operating correctly. Even then, there is no straightforward and clear way for the mechanic to diagnose the problem.

1.4.1 Current Methods

The methods currently used to detect system faults are not very accurate, and as noted earlier, it requires a number of judgment calls by a mechanic. The only measurements that can be taken are: the clutch on and off cycle times and the low and high side pressures. This data is taken while the car is in steady-state condition. That is, the car is idling; therefore, the compressor rpm and condenser air flow are constant. However, there is no consideration of the condenser air temperature, evaporator air temperature, or the type of vehicle. A refrigerant manifold gauge set is connected to the service ports on the high and low pressure sides of the system, and this can be used to measure the maximum and minimum pressures that occur while the system is cycling.

The mechanic can record the on and off cycle times, the length of time that the clutch is either engaged or disengaged. The gathered information is then compared to cycle time and pressure data given in charts in the repair manual. The acceptable range of values is very large, and the mechanic must decide whether or not the system is low on charge based on these rough charts. It is obvious from the wide range of acceptable values that this is not an exact science. The large acceptable area means that the system could be quite low on refrigerant and still fall within the accepted region.

1.4.2 Possible Approaches to On-line Charge Loss Detection

As discussed earlier, the object of this study is to develop a diagnostic method using information that is already available or information that would be very inexpensive to measure. The cycle time of the clutch is already in use by mechanics. Thus, this parameter merits study. Some systems measure the high side pressure, but the CCOT systems discussed in this paper do not continuously measure pressure anywhere in the loop. The pressure at the evaporator outlet is known when the clutch engages and disengages due to the mechanical pressure cutoff switch; therefore, some pressure data is available.

1.5 Current Methods for On-line Charge Loss Detection.

Currently there is no good, reliable on-line method available for detecting charge loss. On-line warning sensors for other faults, such as the engine overheating is standard, but no such standard has been developed for the air conditioning system.

1.5.1 Liquid-Gas Flow Ratio Charge Loss Detector

A group from Nippondenso Co., Ltd, developed a method for monitoring the level of refrigerant in an automotive air-conditioning system [4]. Their idea was to measure the ratio of vapor to liquid upstream of the expansion device, and this ratio would allow them to determine the amount of refrigerant in the system. The research was based on a system with a receiver between the condenser and expansion valve. The purpose of the receiver is to hold excess refrigerant and ensure that liquid refrigerant proceeds to the expansion valve. Any gaseous refrigerant from the condenser is caught in the receiver. As the refrigerant charge is reduced, the liquid level in the receiver is reduced and vapor bubbles begin to enter the line to the expansion valve. A chamber was constructed and

placed in series with the refrigerant line, and some refrigerant was diverted into the chamber where the liquid and gas can separate. The liquid level is sensed by a float switch which turns on a warning light when the liquid level drops too low.

The method described above has several disadvantages. It does not detect charge loss until approximately 60% of the charge has been lost. It is questionable whether or not any damage has occurred to the system at this point. Also, the impact on the environment would be quite large. Including such a chamber in the air-conditioning system will increase the overall cost. Including such a device in the system would require more refrigerant, hose, and fittings. As discussed earlier, the extra hose and fittings will only increase the amount of charge being lost. The method is only applicable to one particular type of system. For example, it is unclear if it will work with an A/C system that has an accumulator on the low pressure side, between the evaporator and compressor. This type of device also assumes that no other system fault will result in vapor exiting the receiver.

1.5.2 Other Detection Devices.

Published material on refrigerant charge loss detection devices and methods is very scarce. Some methods have been tried that, in part, used the clutch cycle time, but none have been successful so far.

1.6 Review of Automotive Refrigerants.

Prior to this decade, R-12 (also known as CFC-12) had been the refrigerant of choice since the introduction of automotive air conditioning.

> "CFC-12 has been the refrigerant of choice due to its unique properties. These include low toxicity, nonflammability, good stability and materials compatibility, oil solubility, as well as good thermodynamic properties." [5]

However, once CFCs (chlorofluorocarbons) were tagged as a major factor in the depletion of the ozone layer, a replacement had to be found. Research and testing occurred throughout the 1980's, and a group of HFC refrigerants was developed. Of this family of refrigerants, HFC-134a, R-134a, was determined to be the best replacement for R-12. R-134a has many of the same qualities that made R-12 desirable, but the impact of

R-134a on the environment is drastically less than that of R-12. Since 1992, R-134a has become the new automotive refrigerant of choice.

Some of the saturation properties of R-134a are given below in Table 1.1 over a small range of temperatures and pressures [6].

Table 1.1 Saturation Properties for R-134a.

Temperature	Pressure	Density		Enthalpy	
		Liquid	Vapor	Liquid	Vapor
(°F)	(Psia)	(lb/ft^3)	(lb/ft^3)	(Btu/lb)	(Btu/lb)
26.00	37.7	81.424	0.80142	20.02	106.38
28.00	39.3	81.201	0.83360	20.66	106.67
30.00	40.9	80.976	0.86681	21.29	106.96
32.00	42.6	80.750	0.90105	21.94	107.24

A wide range of saturation properties, as well as other R-134a property data, can be found in [6]. As an example, we will look at the refrigerant saturation temperature at the evaporator outlet. For the A/C system that is currently in the lab, the low pressure setpoint that disengages the clutch is 25 psig at the evaporator outlet, and this corresponds to 39.7 psia in Table 1.1. Interpolation results in a saturation temperature of 28.50 °F. At this point the refrigerant temperature is below the freezing point of water; therefore, any water that is condensing on the air side of the evaporator will begin to freeze. The pressure is not allowed to drop any lower than 25 psig in order to avoid excessive evaporator frosting.

The example given above is for pure refrigerant, but in an automotive system the oil used to lubricate the compressor circulates with the refrigerant. Grebner notes that,

> "The presence of oil in a refrigeration system affects the saturation pressure-temperature relationship of the refrigerant due to the solubility of the refrigerant in the oil." [7]

The oil used in our system is a polyalkylene glycol (PAG) synthetic oil. For a given pressure, the oil causes a slight increase in the saturation temperature of the refrigerant-oil mixture. The amount of increase depends on the amount of refrigerant in the liquid mixture, but since this is not measured in our test facility, the exact impact of the oil cannot be calculated. As you will see later, tests from our facility show that the presence

of oil causes approximately a 2 °F increase in the saturation temperature for a pressure of 25 psig. Thus, the saturation temperature at the evaporator outlet is approximately 30.5 °F at the end of the cycle. This saturation temperature will fluctuate slightly due to small fluctuations in the refrigerant quality.

2. EXPERIMENTAL FACILITY DESCRIPTION.

2.1 Overview.

All of the data reported in this document was acquired using the mobile air conditioning test facility located at the University of Illinois at Urbana-Champaign. The lab is in room 115K of the Mechanical Engineering Laboratory. The facility was designed to simulate an automotive air conditioning system as well as the environment surrounding the system. One of the challenges of building such a facility is the dynamic nature and environment of an automotive air conditioning system. With a stationary refrigeration unit, such as a refrigerator or residential air conditioner, many of the parameters are fixed. For instance, the compressor speed is constant, and the air flow across the condenser and evaporator are fixed as well. With an automobile, this is not the case. The compressor is mechanically linked to the engine, and the compressor's speed changes proportionally with changes in the engine rpm (revolutions per minute). The condenser air flow changes as the speed of the vehicle changes and as the cooling fan switches on and off. Such dynamic changes are unavoidable; therefore, a facility designed to simulate such a system must be able to simulate these dynamic situations.

Numerous details on the design and construction of the test facility can be found in Weston [8] and Rubio-Quero [9]. Some modifications to the facility, including a new data acquisition system, were performed by Collins [10]. The main subsystems of the test facility are:

1.) Condenser air flow loop
2.) Evaporator air flow loop
3.) Refrigeration loop
4.) Data acquisition system, and
5.) Environmental control system

Since the three references above describe the test facility in great detail, I will only briefly describe each subsystem listed. However, a few modifications and additions have occurred over the past year, and I will present these changes in a little more detail. Figure 2.1 gives an overall schematic view of the test facility, and it shows the basic layout of the facility, the major subsystems, and the subsystem interconnections.

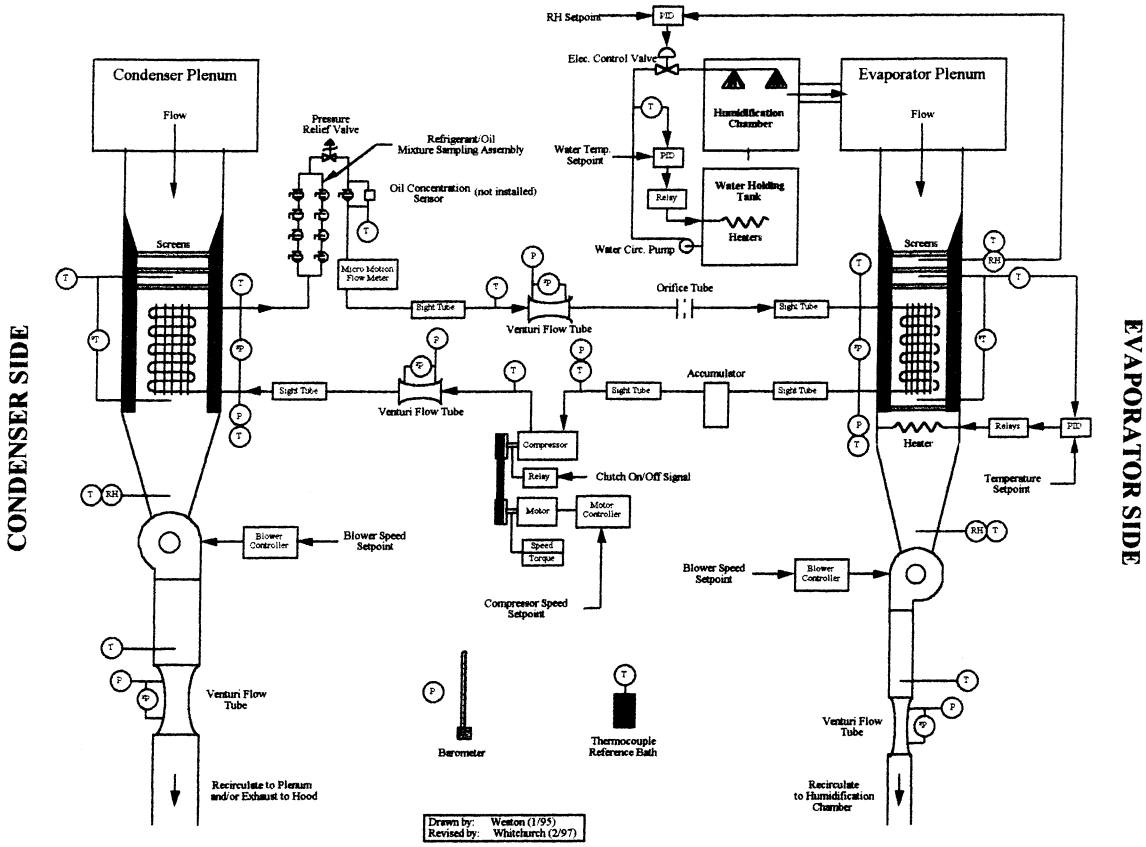

Figure 2.1 Mobile A/C Test Facility Schematic

2.2 Condenser Air Loop.

To simulate the air flow across the condenser, a type of wind tunnel had to be designed to force the air through the condenser. This was accomplished by constructing a closed loop system for the condenser air flow. A rectangular housing surrounds the condenser, and a plenum, a large chamber used to receive/store air, was built upstream of the condenser to allow the air to stabilize before entering the condenser. The air flow is produced by a 5-hp, belt-driven, squirrel cage, AC induction motor. After leaving the condenser the air returns to the blower. In the past, the only source of heat for the air in the condenser loop was the amount rejected from the refrigerant while the system is operating. The temperature was controlled by adjusting the amount of air that was re-circulated from the condenser outlet to the inlet, and the remaining heated air was rejected into the building's ventilation exhaust system. This method presented several problems. When the amount of re-circulated air is changed, the air flow across the

condenser changes, and the blower motor must be adjusted to counteract the change. Also, if a test calls for a low load on the evaporator and a high condenser temperature, the condenser air may not be able to extract enough heat from the refrigerant in order to reach the higher temperature. Four 14.4 amp, 120 volt heaters were placed in the plenum in order to give us better control over the condenser air flow and temperature.

The mass flow rate of the air is measured using a venturi flow tube. For a detailed discussion of how the flow rate is calculated, refer to [10]. The dry bulb temperature of the air is measured at: (1) the condenser inlet, (2) the condenser outlet, (3) the relative humidity probe, located upstream of the condenser, and (4) the venturi inlet. The condenser inlet is measured with a 9-point thermocouple array, and the outlet is measured with a 40-point thermocouple array. This method gives us a good average of the air temperature flowing through the condenser. It is especially important to use an array scheme at the condenser outlet because the refrigerant temperature drops as it passes through the condenser. The changing refrigerant temperature results in a non-uniform increase in the air temperature exiting the condenser. Thus, measuring the temperature at only one or a few spots would not give an accurate representation of the actual change in air temperature. The temperature taken by the humidity probe is a resistance temperature detector (RTD), and it is used to calculate the humidity ratio of the moist air. The measurement at the venturi inlet is taken with a single thermocouple, and this temperature is needed for the mass flow rate calculations. The air pressure is measured just upstream of the venturi flow tube with a gage pressure transducer. The relative humidity is measured using a thin-film capacitive sensor, and the data is used to calculate properties of the moist air.

2.3 Evaporator Air Loop.

The evaporator is housed in an air duct system similar to the condenser loop, again, see [8] for details on the construction of the duct. The air flow is produced by a 1-hp, direct-driven, AC-induction motor. Like the condenser loop, the air flow rate can be varied over a wide range by adjusting the motor speed. There are three main differences between the condenser and evaporator loops. The evaporator loop: (1) has enough heating capacity to control its temperature, (2) is a closed system (the air is totally re-

circulated), and (3) the humidity can be controlled. A 7-kW heater provides the necessary load for the evaporator, and it provides control for the air temperature. As discussed earlier, this heater provides much of the heat necessary to control the condenser air temperature.

During the summer and fall of 1996 a humidity control system was added to the evaporator loop by Whitchurch [11]. Before this addition the humidity would start out at the ambient humidity and quickly be pulled down to a value of 15 to 20% relative humidity. The air loop was redesigned so that the air would pass through a large chamber where a fine mist of warm water could be sprayed into and mixed with the air. PID controllers regulate the temperature of the water and the water flowrate being sprayed into the chamber. The humidity can now be controlled over a range of 12 to 95% RH. These upper and lower bounds may change slightly depending on the values of the other system parameters such as evaporator air inlet temperature.

2.4 Refrigerant Loop.

As mentioned before, the facility currently consists of a 1994 Crown Victoria air conditioning system: condenser, evaporator, compressor, orifice tube, and accumulator. Most of the rubber hoses that are used in the car to connect the components have been replaced with copper tubing. This was necessary in order to instrument the refrigerant lines because it would be practically impossible to add the many fittings needed for the instrumentation into the rubber lines. Adding the instrumentation caused the lines to be longer than normal, but the overall line lengths were kept as short as possible . As you will see later, the overall system size and optimum refrigerant capacity is close to the actual system. Detailed drawings of the refrigerant loop can be found in [8]. Some modifications were made during the summer of 1996, and details on the changes can be found in Wandell [12].

As with the air loops, the temperatures and pressures are measured up and downstream of every major component. The flow rate of the refrigerant is also measured at three different locations by two venturi flow tubes and a Micro Motion flow meter. An oil sampling section consists of two parallel line segments that can be valved off and removed from the system, and this allows us to measure the amount of oil circulating in

the system using a cascade impacter. The parallel design allows the system to remain in operation while a sample has been removed for testing. An electronic oil sensing device has also been placed in the refrigerant loop [12]. In-line sight glasses allow the user to observe the state of the refrigerant and oil in the system as it circulates. This can be a very useful tool because you do not have to guess whether the refrigerant is sub-cooled, two-phase, or superheated.

2.5 Data Acquisition System.

2.5.1 Hewlett Packard System.

The main data acquisition system that is currently being used is a Hewlett-Packard (HP) 1300A VXI mainframe, a HP E1326B $5^1/_2$-digit scanning multi-meter, and three HP 1345A 16 channel general purpose multiplexers. This system collects all of the temperatures, pressures, flow rates, speeds, and humidity measurements that are taken in our test facility. HP-VEE software is used to design customized data acquisition programs. These HP-VEE programs are used to control the acquisition, real-time display, and storage of the data.

2.5.2 SOMAT Addition.

The fact that the HP data acquisition system samples at less than 1 Hz became an issue last year. An automotive A/C system is so dynamic that such a low sampling rate is not fast enough to accurately record the changes in some of the measured system variables. It was desirable to increase the sampling rate for those variables in order to better "capture" the transients in the data; therefore, I added an additional data acquisition system in the summer of 1996. The unit is a SOMAT 2500 series data acquisition system, and we are using it to sample the data at 100 Hz. Only six channels are currently being used:

1) Clutch signal, to determine clutch engagement/disengagement.
2) Evaporator refrigerant outlet temperature.
3) Evaporator refrigerant outlet pressure.
4) Time.
5) Signal to HP system to indicate that the SOMAT is taking data.
6) Compressor Torque.

The SOMAT system is a secondary acquisition system; therefore, it is not always used. The SOMAT is only used when cycling data is needed. Otherwise, the data from the HP system is adequate.

The evaporator refrigerant outlet temperature is measured using an OMEGA type "T" copper-constantan 304SS sheath, grounded, 6 in. X $^{1}/_{16}$ in. thermocouple (part # GTMQSS-062G-6). The thermocouple has a range of -256 to 752 °F ± 0.9 °F. The thermocouple takes its measurements in the center of the refrigerant flow, and it measures a voltage which must then be converted to temperature using the following equation:

$$T_c = a_0 + a_1 V_t + a_2 V_t^2 + \ldots + a_7 V_t^7$$

where:

T_c = The temperature in degrees Celsius.
V_t = The voltage measured by the thermocouple.
a_i = The polynomial coefficients unique to each type of thermocouple.

The polynomial coefficients for a type T thermocouple are [13]:

$a_0 = 0.10086091$
$a_1 = 25727.94369$
$a_2 = -767345.8295$
$a_3 = 78025595.81$
$a_4 = -9247486589$
$a_5 = 6.97688 \times 10^{11}$
$a_6 = -2.66192 \times 10^{13}$
$a_7 = 3.94078 \times 10^{14}$

Since English system units are used in this thesis the temperatures are then converted from Celsius to Fahrenheit. Instead of using an ice bath to correct for the emf error, an OMEGA miniature cold junction compensator (model MCJ-T) was placed in-line.

The clutch voltage is detected by a voltage divider placed in parallel with the clutch coil. The voltage is measured across a small resistor to determine when the clutch is engaged. The evaporator refrigerant outlet pressure reading is taken directly from the terminals on the pressure transducer. The purpose of the signal sent to the HP data acquisition system is to allow the data from the two systems to be matched up with respect to time and compared, if necessary.

2.6 Environmental Control System.

As discussed earlier, the environment that the automotive A/C system resides in is very dynamic; therefore, the experimental lab must be able to simulate the dynamic situations experienced by the car. There is no central control system for the entire facility. The evaporator humidity system and evaporator air heater have separate closed loop control units. The percent relative humidity, temperature of the humidity water tank, and the evaporator air temperature are all controlled by individual PID controllers which can also be used in a manual mode. An Allen-Bradley programmable logic controller provides control for the condenser and evaporator blower units, compressor drive motor, and compressor clutch. The Allen-Bradley controller is accessed through a PC located in the lab.

3. REFRIGERANT CHARGE OPTIMIZATION.

3.1 Overview.

The word "optimization" in this situation needs some interpretation. To most people the word optimization refers to the act of minimizing or maximizing something. For example, with a residential air-conditioning system, the term optimization could mean maximizing the coefficient of performance of the system. With an automotive air-conditioning system, optimization is not so clearly defined. For an orifice tube, fixed displacement compressor system, the goal of the design engineer is to always have two-phase flow leaving the evaporator. If the refrigerant charge is too low, the system performance will decrease. This condition reduces the amount of heat that the system can remove from the cabin, and the compressor begins to get an insufficient amount of lubricating oil since this oil is carried throughout the system by the refrigerant.

To ensure that the refrigerant will remain in the two-phase region under almost all conditions, an industry standard is to add approximately 10% more refrigerant from the point where the evaporator inlet and outlet refrigerant temperatures cross, approximate saturation point. This also allows the automotive manufacturer a small "safety" reserve.

3.2 Test Conditions and Method.

Automotive air-conditioning systems are designed to rapidly cool down a vehicle cabin during startup. A typical situation is when a car has been sitting for several hours in the hot sun, and the driver turns on the air conditioning system immediately after starting the engine. The driver, and consequently the automotive company, wants the cabin to cool off quickly for obvious comfort reasons. To ensure rapid cooling, two-phase flow needs to be leaving the evaporator even under these extreme conditions.

The test conditions were set based on a common industry standard for the conditions that exemplify an extreme load on a vehicle. Using the specific data for the 1994 Crown Victoria, the conditions in Table 3.1 were chosen as the charge optimization test conditions.

Table 3.1 Test Conditions for Charge Optimization Tests.

Parameter	Units	Setting
Condenser Air Flow	(cfm)	1800
Condenser Air Temperature	(°F)	110
Evaporator Air Flow	(cfm)	220
Evaporator Air Temperature	(°F)	110
Compressor Speed	(rpm)	1950

The charge optimization test method is basically the same as that previously performed in [10]. We started with an evacuated system. The system had been under vacuum for several days to ensure that all of the old refrigerant had vaporized out of the oil. Based on past testing of the system, the optimum refrigerant charge was expected to be close to three lbs; therefore, the system was initially charged with 2.65 lbs. Based on the industry test plan, we are seeking the point where the refrigerant temperature at the evaporator inlet and outlet are equal. The system was allowed to come to steady-state while the data was being recorded. If the refrigerant temperature at the evaporator outlet was greater than at the inlet, a small increment of charge was added. This process was continued until the two temperatures had crossed.

3.3 Optimization Results.

The results of the tests are shown in Figure 3.1, and as can be seen, the refrigerant temperatures first cross over at a charge level of 2.74 lbs. We added refrigerant past this point in order to ensure that the temperature crossing at this point looked reasonable. Also, taking data at higher charge levels would allow us to compare other system variables, such as the coefficient of performance versus refrigerant charge. When looking at the data, the temperatures at 2.67 and 2.85 lbs do not seem to fit well. Further analysis of the data revealed that the condenser air inlet temperature was higher for the 2.85 lbs and lower for the 2.65 lbs tests than what was prescribed in Table 3.1 , and the result was slightly skewed temperatures at the evaporator inlet and outlet. Theoretically, the point where the inlet and outlet temperatures cross represents the saturated vapor point (no superheat), but due to the small pressure drop across the evaporator, there is still a small amount of superheat. After adding the specified amount of refrigerant past where the temperatures cross in order to ensure that the system is

operating under saturated conditions, the resulting optimum refrigerant charge is 2.95 lbs. For all of the remaining tests this value is used as the optimum or "full" charge of the system.

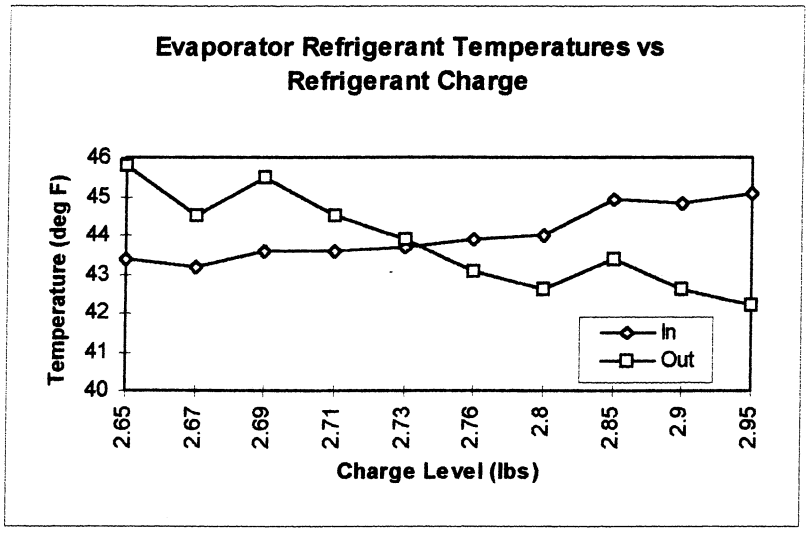

Figure 3.1 Evaporator Inlet and Outlet Refrigerant Temperatures vs. Refrigerant Charge.

As noted earlier, we were interested in how the coefficient of performance (COP) of the system changed as the charge was increased. As it turns out, the COP is maximized at 2.90 lbs, just below the "optimum" 2.95 lbs. It is interesting to note that the COP barely changes over the entire range of refrigerant charge tested The COP at 2.65 lbs is almost the same as the COP at 2.90 lbs. However, requirements for other system variables, such as capacity, may not be met at the 2.65 lbs charge level. In complex systems, such as an automotive air conditioning system, there are a number of variables that need to be optimized simultaneously. Simply optimizing one condition, such as COP, may hinder the system from meeting some other specification, such as a quick pulldown or necessary oil flow requirement.

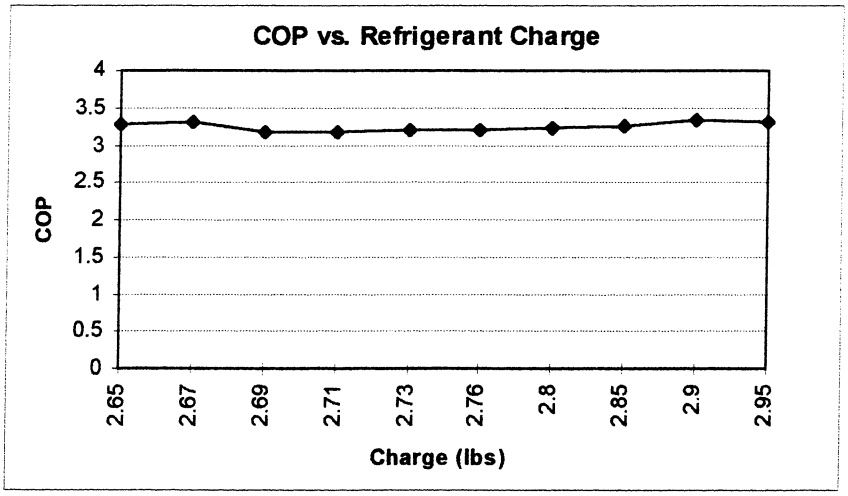

Figure 3.2 System COP vs. Refrigerant Charge.

4. CLUTCH CYCLE TIME AS CHARGE LOSS TOOL.

As discussed earlier, the clutch cycle time is already used by mechanics as a method of detecting low refrigerant charge. As the refrigerant charge is reduced, the on and off portions of the cycle time become shorter. The cycle time of the system is an easy measurement to obtain. It would not involve the expense of a sensor, and it would require minimal computing power. The data would not have to be converted or filtered in any way. It is known that low charge causes shorter cycle times, but the question is what other parameters affect the cycle time and by how much? For example, the temperature of the air, the environmental temperature, is constantly changing. Does this cause a change in the clutch cycle time as well? If it does, can this change be distinguished from the change caused by low charge?

4.1 Previous Work by Collins.

In the spring of 1996 Charles Collins began performing some tests in our facility in order to determine what parameters affect the cycle time and the significance of these effects [10]. It was determined that the system parameters that could have an affect on the cycle time are:

1. Condenser air flow rate
2. Condenser air temperature
3. Evaporator air inlet temperature
4. Refrigerant charge level
5. Compressor speed
6. Evaporator air flow rate
7. Evaporator inlet air humidity

The transient nature of the vehicle and the environment cause these parameters to change constantly. The evaporator air flow rate is ignored during this analysis in order to simplify the tests. It is highly probable that the evaporator air flow rate affects the cycle time, but it could be easily controlled by the vehicle's computer bus. By setting the air flow to a predetermined value, the effect of this parameter can be neutralized. The evaporator inlet air humidity was also left out of the design matrix, and the reasons for this are discussed in section 4.2. Collins used a fractional factorial design matrix to create the tests to be performed. A detailed discussion of fractional factorial design matrices can be found in [14] and [15]. The values for the parameters are given in Table

4.1. These values represent the reasonable environmental conditions and system performance for a 1994 Crown Victoria.

Table 4.1 Parameter Values for Collins' Experimental Design

Tag	Parameter		High	Low
1	Condenser Air Flow	(cfm)	1800	1600
2	Condenser Air Temp	(°F)	110	100
3	Evaporator Air Temp	(°F)	70	65
4	Refrigerant Charge	(lbm)	2.85	2.55
5	Compressor Speed	(rpm)	2800	2500

For a full factorial design matrix, a 2^5 design results in 32 tests, and this represents every possible combination of the high and low values. Since Collins used a half fraction design, he only performed 16 tests, half of the maximum amount. Not performing all of the possible combinations takes less time and resources, but it can cause problems that will be discussed later. The main and interaction effects from his 16 tests are given in Table 4.2.

Table 4.2 Collins' Main Effects and Interactions.
Mean period = 33.1 seconds

1 =	-0.07
2 =	8.38
3 =	6.36
4 =	14.07
5 =	-0.07
12 =	-0.56
13 =	-0.20
14 =	1.42
15 =	5.03
23 =	10.06
24 =	6.32
25 =	-2.77
34 =	3.16
35 =	5.29
45 =	0.96

As can be seen in the table, the refrigerant charge level had the highest impact on the cycle time with a 14.07 second decrease in the cycle time for a 10% loss in charge. The condenser and evaporator air inlet temperatures also had a significant main effect, and several of the two-factor interaction effects were significant including the 15, condenser air flow-compressor speed, effect. The significance of the 15 effect is somewhat suspicious because neither the 1 or 5 main effect was significant; so, can the 15 effect really be that large? It is possible, but it is more likely that confounding has occurred. Since a full factorial design matrix was not performed, the lower order effects are confounded with higher order interaction effects; therefore, one cannot truly tell what parameter(s) caused the change in cycle time. In this case, the 15 interaction is confounded with the 234 interaction effect. It is usually assumed that the lower order effect causes the change, but this is not always true. Since the 2, 3, and 4 main effects had by far the largest impact, it is probable that the 5.03 second difference is due to the 234 instead of the 15 interaction effect.

Two of the 16 tests consisted of long and inconsistent cycling, and this data had a significant impact on the values of the effects. Neutralizing the effect of these two sets of data reduces the 2, 3, and 4 main effects by more than 50%. It was also determined that the orifice tube in the system was not the correct size, and all of the tests were performed under dry evaporator conditions (low humidity). To gain more confidence in the results, more testing and analysis was needed.

4.2 Further Cycle Time Testing.

For the reasons just discussed in section 4.1, it was determined that I should start by performing a full factorial design matrix in order to resolve these issues. We decided to use the same five parameters for the design matrix, and this resulted in $2^k = 2^5 = 32$ tests to be performed. Note that humidity was not included in the design matrix. There are several reasons for this. Including humidity would have doubled the number of tests to be performed from 32 to 64. If one wanted to include humidity in the resulting equation for the cycle time, humidity would need to be included in the matrix. However, humidity is very difficult and expensive to measure; therefore, it was not included. It

was felt that the impact of humidity could be determined from a smaller set of tests, and this will be discussed in detail later.

4.2.1 2^5 Design Matrix.

A 2^k full factorial design matrix was implemented using the same five parameters that Collins used in his tests. The values for the parameters are given in Table 4.3.

Table 4.3 Parameter Values for 2^5 Experimental Design Matrix.

Tag	Parameter		High(+)	Low(-)
1	Condenser Air Flow	(cfm)	1850	1675
2	Condenser Air Temp	(°F)	110	100
3	Evaporator Air Temp	(°F)	70	65
4	Refrigerant Charge	(lbm)	2.95	2.65
5	Compressor Speed	(rpm)	1950	1700

The values for the temperatures are the same as in Table 4.1, but the other parameter values have changed slightly. The refrigerant charge has increased slightly, as was discussed in section 3.3. The condenser air flow and compressor speed data have changed because more accurate data was obtained for the 1994 Crown Victoria system. The test matrix and the cycle time results are given in Table 4.4.

Two examples of the test data are shown in Figure 4.1. Only the evaporator outlet refrigerant pressure and a representation of the clutch voltage are shown. The lower, square, wave represents the clutch voltage with the high level indicating that the clutch is engaged. Note that the clutch disengages when the evaporator outlet refrigerant pressure reaches the low pressure set point of 25 psig. From a quick inspection of the graph, there does not seem to be a significant difference in the cycle times between the full and 10% low charge tests. Table 4.4 can be rather difficult to interpret; so, in order to make it a little easier to see the impact of the various parameters on the cycle time, the (+) and (-) groups of data for each parameter are averaged and given, along with the standard deviations, in Table 4.5.

Table 4.4 2^5 Test Matrix and Cycle Times.

Test	Parameter					Cycle	Std Dev
	1	2	3	4	5	Time (sec)	(sec)
1	-	-	-	-	-	30.01	0.79
2	+	-	-	-	-	29.75	1.71
3	-	+	-	-	-	32.75	1.51
4	+	+	-	-	-	29.47	0.88
5	-	-	+	-	-	29.27	1.11
6	+	-	+	-	-	27.04	1.13
7	-	+	+	-	-	32.32	0.75
8	+	+	+	-	-	27.72	6.51
9	-	-	-	+	-	30.33	1.12
10	+	-	-	+	-	31.16	0.85
11	-	+	-	+	-	34.79	3.32
12	+	+	-	+	-	31.03	0.87
13	-	-	+	+	-	31.42	2.13
14	+	-	+	+	-	31.34	2.71
15	-	+	+	+	-	38.71	5.39
16	+	+	+	+	-	33.19	4.92
17	-	-	-	-	+	31.25	2.98
18	+	-	-	-	+	32.11	0.68
19	-	+	-	-	+	28.76	1.89
20	+	+	-	-	+	27.28	1.83
21	-	-	+	-	+	29.52	1.70
22	+	-	+	-	+	29.97	1.34
23	-	+	+	-	+	28.01	3.36
24	+	+	+	-	+	32.38	0.69
25	-	-	-	+	+	27.90	1.60
26	+	-	-	+	+	28.92	0.95
27	-	+	-	+	+	32.41	2.60
28	+	+	-	+	+	31.44	2.95
29	-	-	+	+	+	30.03	1.66
30	+	-	+	+	+	38.95	4.03
31	-	+	+	+	+	31.40	2.45
32	+	+	+	+	+	32.66	1.49
			Average			31.04	2.76

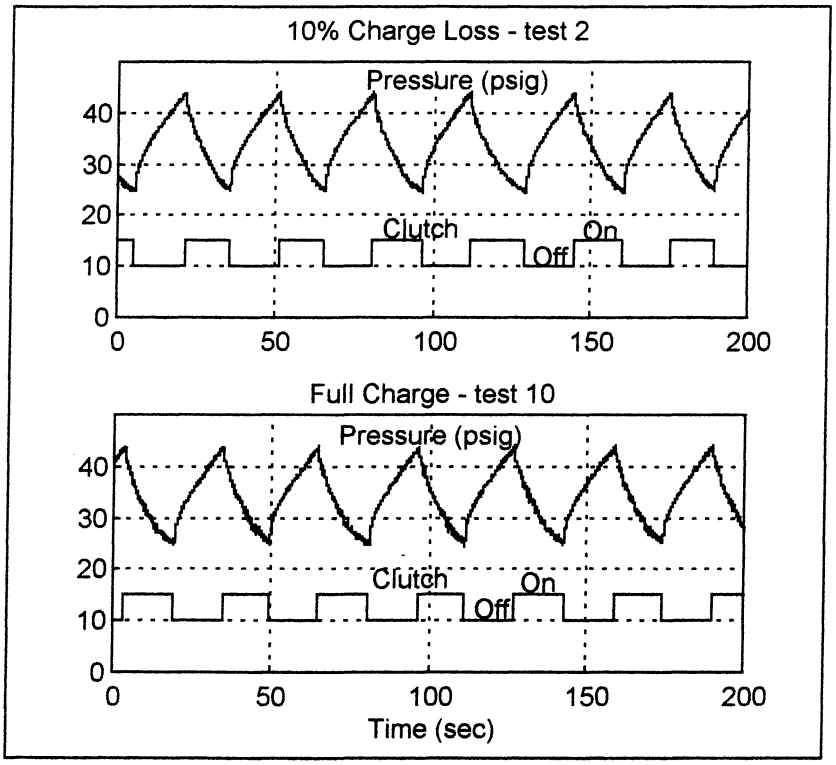

Figure 4.1 Examples of data used to collect the clutch cycle times. Note: the refrigerant pressure is measured at the evaporator outlet.

Table 4.5 Analysis of Parameter Effect on Cycle Time.

	Average(sec)	Std Dev(sec)
All Tests	31.04	2.76
Cond Air Flow (+)	30.90	2.87
Cond Air Flow (-)	31.18	2.73
Cond Air Temp (+)	31.52	2.91
Cond Air Temp (-)	30.56	2.60
Evap Air Temp (+)	31.50	3.40
Evap Air Temp (-)	30.58	1.94
Ref. Charge (+)	32.23	3.04
Ref. Charge (-)	29.85	1.87
Comp Speed (+)	30.81	2.79
Comp Speed (-)	31.27	2.80

Notice that in the cases of condenser and evaporator air inlet temperatures and refrigerant charge, a parameter increase resulted in an increase in cycle time. However, for the condenser air flow and compressor speed, an increase of the parameter caused a

decrease in the cycle time. From a physical standpoint none of these results come as a surprise. A higher condenser air flow will increase the heat transfer rate (removing more of the load from the system), and the temperature and pressure will drop quicker. A faster drop in pressure results in a shorter cycle time because the cycle ends when the pressure drops down to the low pressure cutoff value. A higher condenser air temperature will reduce the heat transfer rate across the condenser, and it will take longer for the system temperature and pressure to drop. An increase in evaporator air temperature increases the load on the system, and once again this causes a slower drop in the outlet pressure, resulting in a longer cycle time. A higher charge level also increases the cycle time, as expected. When the compressor clutch engages, it quickly begins to remove the refrigerant from the low side of the system causing a decrease in the evaporator outlet pressure. If the system has more charge in it, it will take longer for the pressure to drop, and the system can recover faster because of refrigerant moving from the high side to the low side of the system. An increase in refrigerant will also increase the capacity of the system by increasing the heat transfer rate in the evaporator. These effects will cause a longer cycle time, as shown in the data. Table 4.5 indicates that an increase in compressor speed causes a slight decrease in the clutch cycle time, and this result was also expected. As the compressor pumps faster, the low side pressure will drop faster, and it will reach the low pressure cutoff point of 25 psig quicker. The data indicates that the condenser air flow and compressor speed have very small effects on the clutch cycle time; therefore, it may be possible to ignore these variables when using the cycle time as a charge loss indicator.

It is also important to note the standard deviations of the data. A lot of the deviation is due to the parameter interaction effects that will be discussed in the next section, but the variance of the data may also have a significant impact on the measurements. The interaction effects can be accounted for, but the variance in the data can become a problem.

4.2.2 Statistical Analysis of Cycle Time.

Since the tests that were performed were from a 2^k full factorial design matrix, there is a good bit of statistical analysis that can be conducted with the data. The first

step is to look at the main and interaction effects of the five parameters. Since the test matrix is a full factorial design, confounding of the effects is not a concern. As noted earlier, confounding can occur when every combination of the low and high values for the parameters is not used. See [14] and [15] for more details on confounding. The main, second order, and third order interactions are given below in Table 4.6.

Table 4.6 Main and Interaction Effects for Cycle Time.

	Effect (sec)
Y (average)	31.04
x1	-0.28
x2	0.96
x3	0.91
x4	2.38
x5	-0.46
x1x2	-1.47
x1x3	0.60
x1x4	0.49
x1x5	2.08
x2x3	0.15
x2x4	0.99
x2x5	-1.50
x3x4	1.55
x3x5	0.69
x4x5	-0.58
x1x2x3	0.02
x1x2x4	-0.99
x1x2x5	0.46
x1x3x4	0.33
x1x3x5	1.35
x1x4x5	0.26
x2x3x4	-1.04
x2x3x5	-0.61
x2x4x5	0.08
x3x4x5	-0.07

Of the main effects and interactions listed, the refrigerant charge, x4, has the largest impact on cycle time. However, all five of the main effects, as well as a number of the two and three factor interactions seem to have a significant impact on the system as well. This indicates that the cycle time is quite sensitive to all of the parameters that

were varied during the tests, and it would be necessary to account for all of these parameters in order to build an accurate model for the system cycle time.

Often in two-level design matrices the three factor and higher interactions are assumed to be zero, and any computed value for these higher effects is simply noise in the data. This is only an assumption, however. In our tests it looks like some of the three factor interactions, such as the 234 interaction, are significant; therefore, only the fourth and fifth order interactions are assumed to be negligible, Table 4.7. This data will then be used to estimate the standard error, sample variance, of the effects. The variance is a measure of the variability of the data. In other words, it indicates the amount of noise, uncertainty, in the data.

Table 4.7 Higher Order Interaction Effects for Cycle Time.

Interaction	Effect (sec)
x1x2x3x4	-0.84
x1x2x3x5	0.05
x1x2x4x5	-0.41
x1x3x4x5	0.26
x2x3x4x5	-1.48
x1x2x3x4x5	-0.65

Once computed, the sample variance can be used to help determine which effects and interactions in Table 4.6 are statistically significant. The variance can be estimated with the equation:

$$s^2_{\text{effect}} = \sum_{\substack{\text{higher-order} \\ \text{interactions}}} \frac{\left(E_i - \mu_{E_i}\right)^2}{N_h}$$

where N_h is the number of higher order interactions. Since the interactions of Table 4.7 were assumed to be zero, μ_{Ei} is equal to zero. This results in:

$$s^2_{\text{effect}} = \sum_{\substack{\text{higher-order} \\ \text{interactions}}} \frac{\left(E_i\right)^2}{6} = 0.59$$

Thus, the estimated sample standard deviation , s_{effect}, is 0.77. A confidence interval can now be developed that will allow us to determine the significance of the effects of Table 4.6.

Since the variance was estimated, a student's t-distribution will be used to construct the confidence interval. I want to be 95% confident that an effect is significant and not due to randomness in the data; therefore, from Table A.3 of [14] we have $t_{32,0.975} = 2.038$. This results in:

$E_i \pm t_{32,0.975} * s = E_i \pm (2.038)*(0.77)$

$E_i \pm 1.57$

This means that for us to be 95% confident that an effect is significant, its magnitude must be greater than 1.57. Figure 4.2 gives a graphical representation of these confidence intervals.

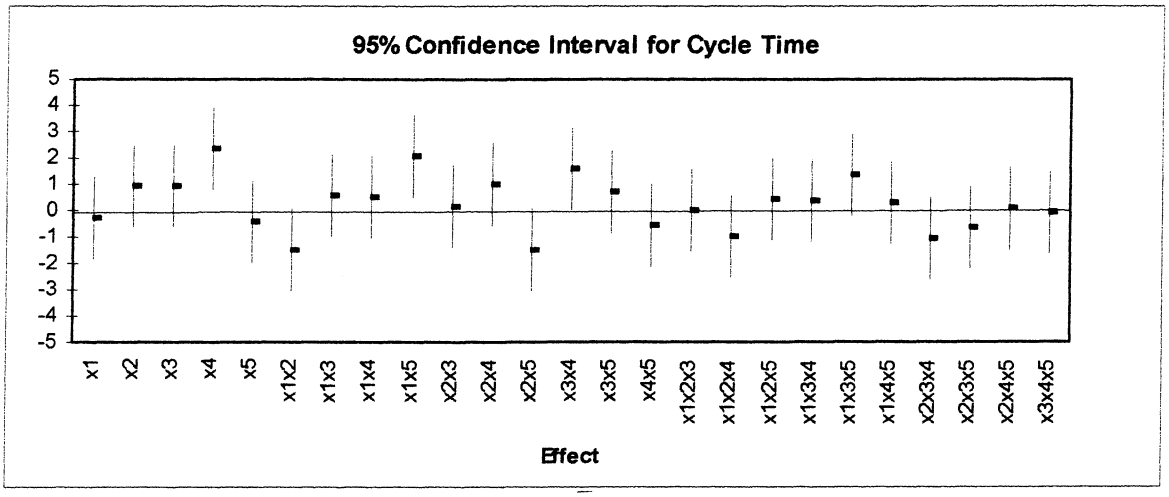

Figure 4.2 95% Confidence Intervals for the Cycle Time Effects.

The dots represent the calculated value of the effect, and the lines represent the confidence interval. Due to the variability of the data, the actual value of the effect could lie anywhere along the line. Thus, if the line crosses the x-axis (i.e. effect = 0), the effect must be assumed to be equal to zero. The only effects that do not cross over zero are x4 and x1x5. The x3x4 value looks questionable from the graph, but Table 4.6 verifies that it does indeed cross over the x-axis. The effects that were found to be significant are listed in Table 4.8 below.

Table 4.8 Significant Effects for Cycle Time-95% Confidence.

	Effect
Y	31.04
x4	2.38
x1x5	2.08

A mathematical model for the system cycle time can now be constructed.

$$CT = Y + b_1*x1 + \ldots + b_{12}*x1*x2 + \ldots + b_{123}*x1*x2*x3 + \ldots + b_{1234}*x1*x2*x3*x4 + \ldots + b_{12345}*x1*x2*x3*x4*x5$$

where $b_i = \frac{E_i}{2}$ and CT = Cycle Time of system.

The basic equation for CT contains 32 terms (31 effects and the average,Y, value), but since we are only confident that the effects of Table 4.8 are significant, the equation will contain only a few terms. Thus, the resulting equation is:

$CT = 31.04 + 1.19*x4 + 1.04*x1*x5$

The final equation for the cycle time is very simple and the refrigerant charge is a significant variable. However, in this case simplicity is not necessarily a good thing. The reason for the simplicity is that almost all of the effects were determined to be statistically insignificant based on the estimated variance and chosen confidence interval. A variance of 0.59 is quite large compared to the largest effect value of 2.38. The fact that most of the effects were left out of the final equation does not mean that they do not have an effect on the cycle time. It just means that there is so much variability, or randomness, in the data that it cannot be determined if the value of the effect is real or if it is simply a result of the data variability.

If every possible term were included in the model, the model would predict the same cycle time as that measured and listed in Table 4.4 (a very small difference would be incurred due to the roundoff of the effect values). To check our model for the cycle time, we will plug in the corresponding +1 or -1 for the parameter variable and compute the cycle times. The results are given in Table 4.9.

Table 4.9 Check of Cycle Time Model-95% Confidence.

Test	Cycle Time (sec)		% Error
	Measured	Predicted	
1	30.01	30.89	2.94
2	29.75	28.81	-3.16
3	32.75	30.89	-5.67
4	29.47	28.81	-2.24
5	29.27	30.89	5.54
6	27.04	28.81	6.54
7	32.32	30.89	-4.43
8	27.72	28.81	3.91
9	30.33	33.27	9.72
10	31.16	31.19	0.10
11	34.79	33.27	-4.36
12	31.03	31.19	0.50
13	31.42	33.27	5.90
14	31.34	31.19	-0.49
15	38.71	33.27	-14.06
16	33.19	31.19	-6.03
17	31.25	28.81	-7.81
18	32.11	30.89	-3.79
19	28.76	28.81	0.18
20	27.28	30.89	13.23
21	29.52	28.81	-2.41
22	29.97	30.89	3.07
23	28.01	28.81	2.86
24	32.38	30.89	-4.58
25	27.90	31.19	11.80
26	28.92	33.27	15.05
27	32.41	31.19	-3.78
28	31.44	33.27	5.82
29	30.03	31.19	3.87
30	38.95	33.27	-14.58
31	31.40	31.19	-0.68
32	32.66	33.27	1.87

As one can see, the predicted values are not very good. Some are close, but several are off by more than 14% from the measured value. In order to more quantitatively measure the effectiveness of the equation fitting, the method of average percent absolute deviation (APD) was applied to the data of Table 4.9. The APD method takes into account the magnitude of the dependent variable being measured [16]:

$$APD = \frac{100}{N}\sum_{i=1}^{N}\sqrt{\left(\frac{Y_i - y_i}{Y_i}\right)^2}$$

where,

Y_i = Measured value for each test.
Y_i = Predicted value for each test.
N = Total number of tests = 32.

After performing the calculations,

APD = 5.34

This means that the fitted equation is on average more than 5% different from the data points that were used to create the equation.

A 95% confidence interval is somewhat restrictive; so, we will look at what happens if one only wants to be 80% confident that an effect is significant. Using the chart found in [14] results in:

$t_{32,0.90} = 1.309$. This gives:

$E_i \pm t_{32,0.90} * s = E_i \pm (1.31)*(0.77)$

$E_i \pm 1.01$

The range of the confidence intervals for the effects are given in Figure 4.3.

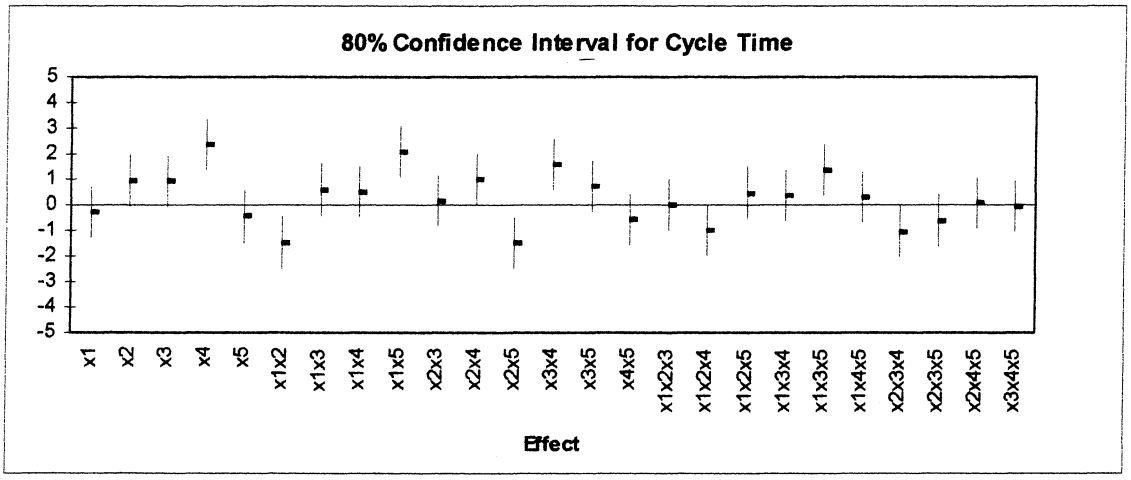

Figure 4.3 80% Confidence Intervals for the Cycle Time Effects.

Note that the points are the same as in Figure 4.2, but now the lines, confidence intervals, are shorter. The lines are now shorter because we decided that we did not need to be as confident about whether or not the magnitude of the effects are truly greater than zero. This results in more effects not crossing over the zero line. The result is that now seven effects are deemed significant, instead of just two terms for the 95% confidence interval. The significant effects are listed below in Table 4.10.

Table 4.10 Significant Effects for Cycle Time-80% Confidence.

	Effect
Y	31.04
x4	2.38
x1x2	-1.47
x1x5	2.08
x2x5	-1.50
x3x4	1.55
x1x3x5	1.35
x2x3x4	-1.04

The resulting equation for the clutch cycle time is not nearly as simple as with the 95% confidence interval:

$$CT = 31.04 + 1.19*x4 - 0.74*x1*x2 + 1.04*x1*x5 - 0.75*x2*x5 + 0.78*x3*x4 + 0.68*x1*x3*x5 - 0.52*x2*x3*x4$$

Instead of only three terms with the 95% confidence interval, the equation now consists of eight terms. This should cause the equation to be in better agreement with the experimental data, and Table 4.11 indicates a better fit.

While the errors look better than in Table 4.9, one error is still over 13%, test 26. Using the APD method described earlier,

APD = 3.82

While this is a significant decrease from the 95% confidence interval analysis, an average percent deviation of almost 4% is still a concern.

Table 4.11 Check of Cycle Time Model-80% Confidence.

Test	Cycle Time (sec)		
	Measured	Predicted	% Error
1	30.01	30.03	0.08
2	29.75	30.76	3.41
3	32.75	31.96	-2.41
4	29.47	29.75	0.97
5	29.27	28.78	-1.66
6	27.04	26.82	-0.79
7	32.32	32.79	1.45
8	27.72	27.89	0.61
9	30.33	29.82	-1.67
10	31.16	30.55	-1.96
11	34.79	33.83	-2.77
12	31.03	31.62	1.89
13	31.42	33.76	7.44
14	31.34	31.80	1.45
15	38.71	35.69	-7.82
16	33.19	30.79	-7.24
17	31.25	30.79	-1.46
18	32.11	33.00	2.77
19	28.76	29.72	3.36
20	27.28	28.99	6.27
21	29.52	26.85	-9.03
22	29.97	31.75	5.94
23	28.01	27.86	-0.51
24	32.38	29.82	-7.88
25	27.90	30.58	9.62
26	28.92	32.79	13.37
27	32.41	31.59	-2.55
28	31.44	30.86	-1.85
29	30.03	31.83	6.00
30	38.95	36.73	-5.71
31	31.40	30.76	-2.05
32	32.66	32.72	0.17

4.3 Current Tests vs. Tests by Collins.

You have probably noticed by now that the results from Collins' data and the data presented in section 4.2 are not in good agreement. For instance, the two, three, and four main effects from Collins' data are much larger than those just presented in section 4.2.2. There are several possible reasons for the differences. As noted earlier, two of the

sixteen tests performed by Collins experienced very long and uneven cycles due to a high load on the system, and these two large values had a significant impact on the effects. If the effect of these two tests are reduced by setting them equal to the third highest cycle time value, the two, three, and four main effects are approximately cut in half. This indicates how sensitive these calculated effects are to only one or two "bad" data sets.

The orifice tube that was used during the tests performed by Collins was determined to be incorrect. The orifice tube used by Collins was a 0.052" diameter type, and our tests used the correct, 0.057" diameter, tube. The smaller tube probably caused some restriction in the flow of refrigerant to the evaporator and a greater pressure drop. The impact of the smaller tube on the cycle time is not obvious, but it could account for some of the differences in the data.

The third difference is the change in optimum refrigerant charge level. Collins determined that the optimum charge was 2.85 lbs, but, using more accurate test parameter information obtained from one of our corporate sponsors, it was determined that the optimum charge was 2.95 lbs. We will now take a closer look at the cycle time response over a wider range of refrigerant charge.

4.4 Cycle Time vs. Refrigerant Charge Level.

The refrigerant charge level was varied from 30% below to 10% above the optimum charge of 2.95 lbs for two different sets of conditions. The conditions for the parameters are given in Table 4.12. The experiments resulted in the average cycle times given in Table 4.13. As expected, the cycle time continues to decrease as the system charge is reduced, and this result is easier to visualize in Figure 4.4 below.

Table 4.12 Test Conditions for Cycle Time vs. Charge Level.

Test	Cond Air Flow (cfm)	Cond Air Temp (°F)	Evap Air Temp (°F)	Compressor Speed (rpm)	Humidity (%RH)
A	1675	100	65	1700	20
B	1850	110	70	1700	20

Table 4.13 Results of Cycle Time vs. Refrigerant Charge Tests.

Ref. Charge	% of	Test A (sec)		Test B (sec)	
(lbs)	Optimum	Cycle	Std Dev	Cycle	Std Dev
2.05	70	20.29	0.28	18.42	0.38
2.35	80	24.81	0.69	24.30	1.64
2.65	90	27.47	1.00	30.85	1.06
2.95	100	28.46	0.86	34.79	1.00
3.25	110	30.67	1.02	32.78	3.17

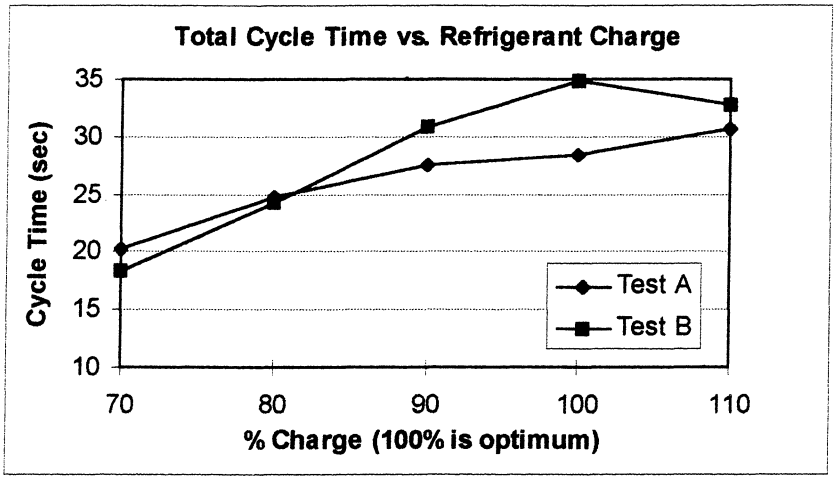

Figure 4.4 Cycle Time vs. Percent of Optimum Charge.

Notice that the change from 100 to 90, representing a 10% loss in charge, is not very significant, but when the charge level drops below 90 the cycle time begins to drop more sharply and in a linear fashion. My tests were performed between 90 and 100% charge, but Collins' tests were performed approximately between 85 and 95% charge. Therefore, Collins' tests were slightly further to the left of the graph where the rate of change in cycle time is greater. This also added to the larger parameter effects found by Collins. It is important to note that detecting the first 10% of charge loss is difficult. The very small decrease in cycle time for the first 10% of charge loss is due to the fact that the system is inherently slightly "overcharged" at the optimum value. This fact can be seen in Figure 4.5 below. For the test conditions of tests 1 and 9 from Table 4.4, the average cycle time is 30.01 seconds for a 10% loss of charge and 30.33 seconds for a full

charge. In two cases found in Table 4.4, the cycle times are actually slightly longer for the low charge tests.

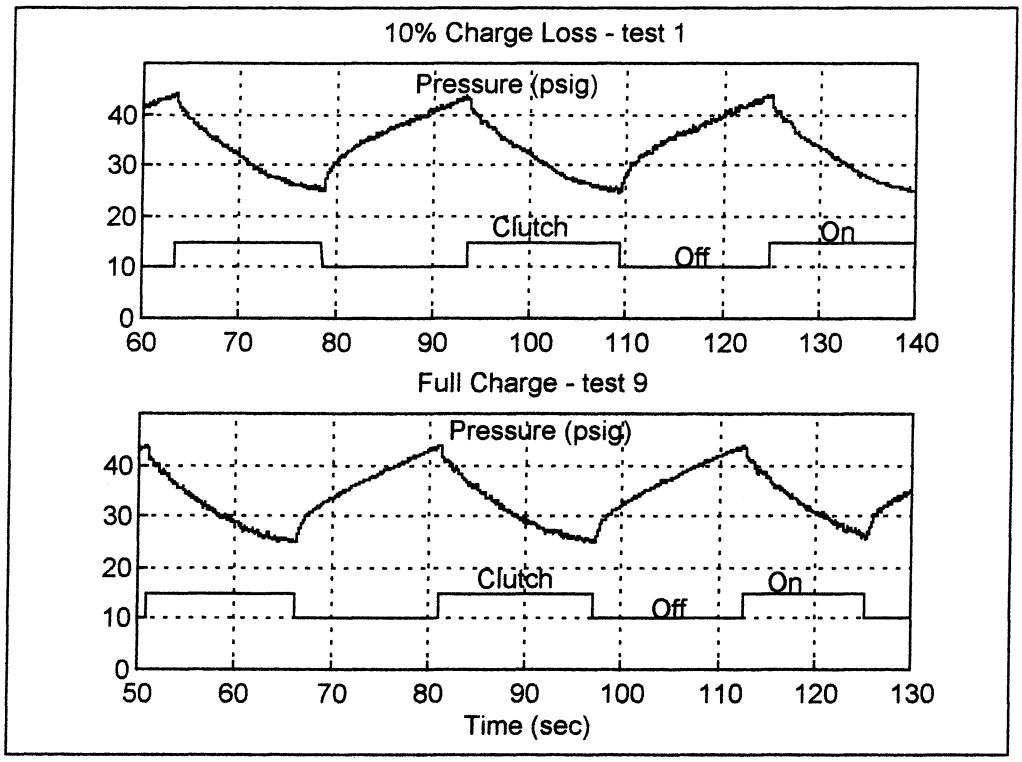

Figure 4.5 Insignificant change in cycle time due to a 10% loss of charge. Note: refrigerant pressure is measured at the evaporator outlet.

4.5 The Humidity Question.

As discussed in the introduction of this chapter, the humidity in the vehicle cabin (hence, the humidity of the air passing through the evaporator inlet) could have a significant impact on the cycle time results.

A set of tests was designed to look at the impact of automotive cabin humidity on the system cycle time. The conditions of the tests are given in Table 4.14. Notice that the conditions for tests A1 through B2 are similar to the experiments performed in section 4.2, but Tests C1 through D2 have a higher evaporator air temperature of 80 and 85 degrees. The tests that end with a "1" indicate a 20% charge loss, and the test names that end with a "2" correspond to a full charge. Each letter (A,B,C,D) corresponds to a different evaporator air inlet temperature. A set of four tests was performed where the

relative humidity varied from 20% to 80% for each set of conditions. The resulting cycle times for the tests are given in Table 4.15.

Table 4.14 Test Conditions for Cycle Time vs. Humidity Experiments.

Test	Cond Air Flow (cfm)	Cond Air Temp (°F)	Evap Air Temp (°F)	Compressor Speed (rpm)	Refrigerant Charge (lbs)
A1	1675	100	65	1950	2.35
A2	1675	100	65	1950	2.95
B1	1675	100	70	1950	2.35
B2	1675	100	70	1950	2.95
C1	1675	100	80	1950	2.35
C2	1675	100	80	1950	2.95
D1	1675	100	85	1950	2.35
D2	1675	100	85	1950	2.95

Table 4.15 Cycle Times for Various Humidity Levels.

Experiment	% Relative Humidity			
	20		40	
	Cycle (sec)	Std Dev (sec)	Cycle (sec)	Std Dev (sec)
A1	28.85	1.58	40.40	1.28
A2	29.79	1.08	50.06	3.22
B1	28.88	2.78	32.72	2.11
B2	28.45	2.49	56.16	3.47
C1	24.95	1.57	25.47	0.97
C2	30.37	4.38	no cycle	---
D1	24.40	1.53	25.13	6.66
D2	69.09	21.17	no cycle	---

Experiment	% Relative Humidity			
	60		80	
	Cycle (sec)	Std Dev (sec)	Cycle (sec)	Std Dev (sec)
A1	32.68	1.08	25.04	2.57
A2	62.71	1.94	no cycle	---
B1	23.47	0.57	32.01	16.31
B2	no cycle	---	no cycle	---
C1	no cycle	---	no cycle	---
C2	no cycle	---	no cycle	---
D1	no cycle	---	no cycle	---
D2	no cycle	---	no cycle	---

As the data indicates, the automobile cabin humidity has a tremendous effect on the clutch cycle time of the A/C system. It is somewhat difficult to follow the data in Table 4.15; therefore, a few plots may help.

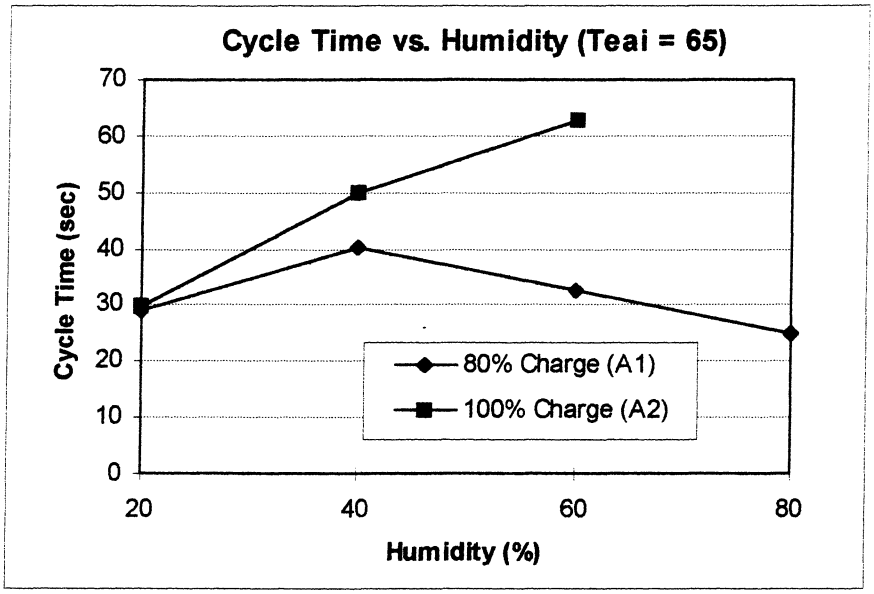

Figure 4.6 Effect of humidity on the cycle time for T_{eai} = 65 °F.

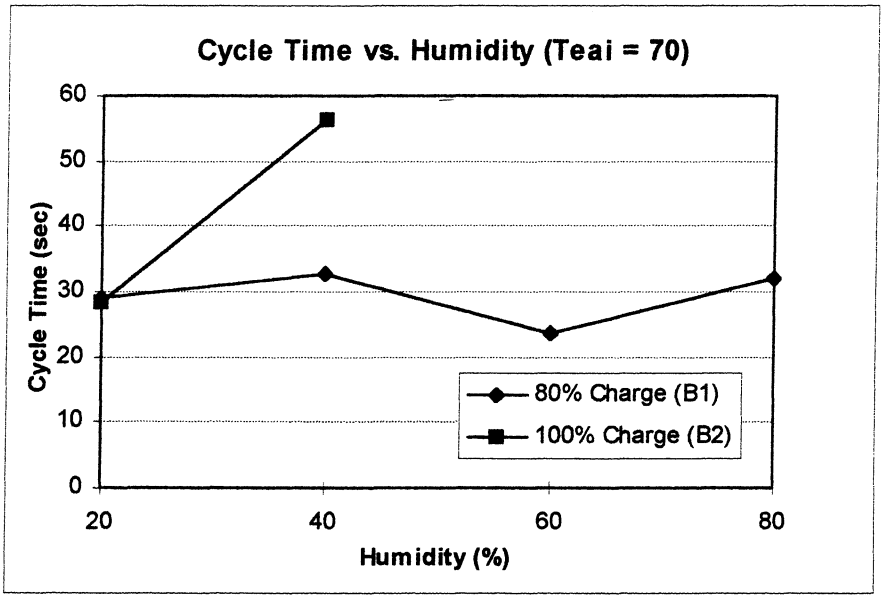

Figure 4.7 Effect of humidity on the cycle time for T_{eai} = 70 °F. Note: Missing data points indicate that the system did not cycle.

First, take a look at the case where T_{eai} = 65 °F. While the plot of A2, full charge, is above that of A1, 20% low charge, it is obvious from Figure 4.6 that it is impossible to detect the 20% loss of charge without knowing what the humidity is. For instance, A1 is much lower than A2 at 40% RH, relative humidity, but A1 at 40% is higher than A2 at 20% RH. For T_{eai} = 70 °F, B1 at 20% humidity cannot be distinguished from B2 at 20% humidity. B1 at 40% and 80% RH is higher than B2 at 20% RH, but B1 at 60% RH is lower than B2 at 20%. In this range of low evaporator air inlet temperatures, the humidity must be known so that it can be accounted for in the analysis of the system cycle time.

Air temperatures of 65 and 70 °F are on the low side of the normal range; so, taking a look at temperatures of 80 and 85 °F will cover the full range of reasonable vehicle cabin temperatures.

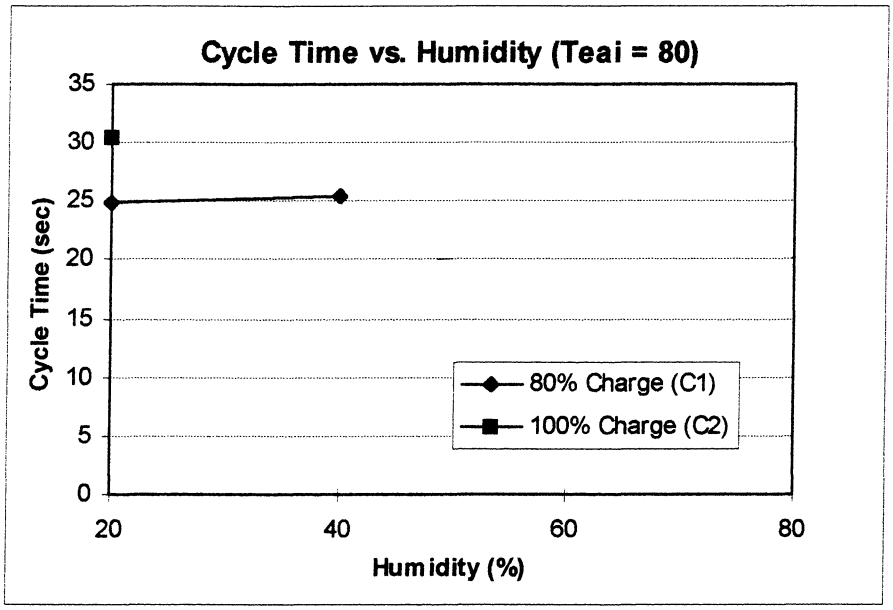

Figure 4.8 Effect of humidity on the cycle time for T_{eai} = 80 °F.

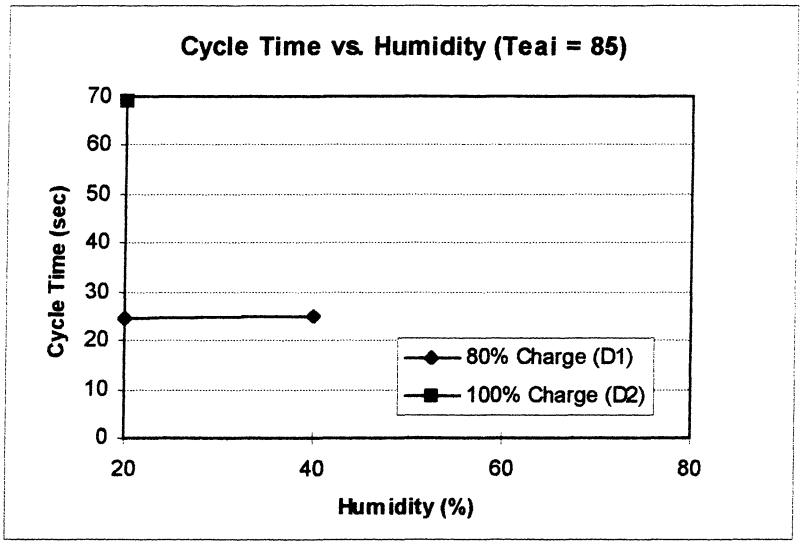

Figure 4.9 Effect of humidity on the cycle time for T_{eai} = 85 °F.

As the evaporator air temperature is increased, the difference in cycle times between full charge and 20% low charge increases, as seen in Figure 4.8, but the system only cycles at low values of humidity. Using the clutch cycle time as a tool for predicting charge loss looks practical for the high cabin temperatures of Figures 5.8 and 5.9. However, the range of parameter values where this is practical has now become quite small. To say that the car cabin temperature must be 80 °F or higher and that the cabin humidity must be below 40% for cycling to occur is quite restrictive. If the vehicle is being operated in a dry climate, this may be practical. The system would see high evaporator air temperatures and low humidity during pulldown. But, in a humid environment, it is quite possible that when T_{eai} is in the 80 to 85 °F range, the humidity will not be low enough to start cycling. When the humidity gets low enough to start cycling, the temperature has dropped below 80 °F. Pulldown tests in our facility have confirmed this hypothesis.

With today's technology and on-board computers it would be possible to force the car cabin to the region described above where the cycle time could be used to detect charge loss. However, the vehicle passengers may not approve of such a method. In a study conducted by [17], it was found that the comfortable range of vehicle cabin temperatures for the summer are between 68 and 78 °F, and this is below the range determined necessary to implement the clutch cycle time method. Studies would need to

be done to determine if several minutes of slightly warmer air in order to perform charge loss tests is acceptable to the average user. At these higher temperatures, the standard deviations of the cycle times are increasing; therefore, data would need to be taken over a longer period of time to ensure that a reliable average cycle time has been computed.

4.6 2^4 Design Matrix Under High Load Conditions.

In section 4.5 we saw that the relative humidity of the air entering the evaporator had a significant impact on the system cycle time, but at high evaporator air temperatures it only cycled at low humidity conditions. In other words, as long as the system is cycling the humidity must be low; therefore, it is not varying and affecting the system. In section 4.5 the only parameters that were varied were evaporator air temperature and humidity. The effect that the other system parameters will have on the cycle time at high evaporator temperatures is not known. To look at the effects of the other parameters a smaller 2^4 design matrix was developed. The high and low values of the parameters are given in Table 4.16. The evaporator conditions are: air inlet temperature = 80 °F and air flow = 220 cfm. Note that the low value of refrigerant charge, 2.35 lbs, represents a 20% loss of charge. From the earlier tests, it seems that detecting a 20% loss of charge using the clutch cycle time may be more practical. The resulting cycle times and standard deviations are given below in Table 4.17. Once again, the average cycle times will be averaged over the (+) and (-) values for each parameter. The resulting data is presented in Table 4.18.

Table 4.16 Parameter Values for 2^4 Experimental Design Matrix.

Tag	Parameter		High(+)	Low(-)
1	Condenser Air Flow	[cfm]	1850	1675
2	Condenser Air Temp	[°F]	110	100
3	Refrigerant Charge	[lbm]	2.95	2.35
4	Compressor Speed	[rpm]	1950	1700

Table 4.17 2^4 Test Matrix and Cycle Times.

Test	Parameter				Cycle	Std Dev
	1	2	3	4	Time (sec)	(sec)
1	-	-	-	-	27.50	1.33
2	+	-	-	-	30.71	1.20
3	-	+	-	-	31.75	1.36
4	+	+	-	-	31.83	1.18
5	-	-	+	-	34.88	0.54
6	+	-	+	-	42.22	9.55
7	-	+	+	-	80.25	17.76
8	+	+	+	-	72.31	10.96
9	-	-	-	+	30.78	0.98
10	+	-	-	+	30.34	1.41
11	-	+	-	+	25.74	1.22
12	+	+	-	+	28.06	1.76
13	-	-	+	+	34.90	1.63
14	+	-	+	+	33.10	0.75
15	-	+	+	+	37.10	10.22
16	+	+	+	+	75.78	15.52
		Average:			40.45	4.82

Table 4.18 Analysis of Parameter Effects on Cycle Time.

	Average(sec)	Std Dev(sec)
All Tests	40.45	18.18
Cond Air Flow (+)	43.04	19.61
Cond Air Flow (-)	37.86	17.55
Cond Air Temp (+)	47.85	23.72
Cond Air Temp (-)	33.05	4.47
Ref. Charge (+)	51.32	20.81
Ref. Charge (-)	29.59	2.22
Comp Speed (+)	36.98	16.09
Comp Speed (-)	43.93	20.52

The loss of refrigerant charge caused a large decrease, 21.73 seconds, in the total cycle time of the system, but the standard deviation of the high charge tests is almost as large as the change, 20.81 seconds. Notice that the other system parameters that were varied caused greater changes in the cycle time than they did at the lower evaporator air

temperatures. The large standard deviations of Table 4.18 are caused by tests 7, 8, and 16. These tests were on the verge of not cycling, and this resulted in very long and inconsistent cycles. The raw data of Figure 4.10 gives examples of why the cycles can be so inconsistent. Once the clutch is engaged, the pressure drops in an exponential manner toward the cutoff value of 25 psig. At higher load conditions the pressure curve will flatten and hover just above the cutoff point. The pressure will oscillate slightly, and at some point one of these oscillations will drop just below 25 psig and end the cycle. Such a pattern results in varying lengths of the "on" and total cycle times.

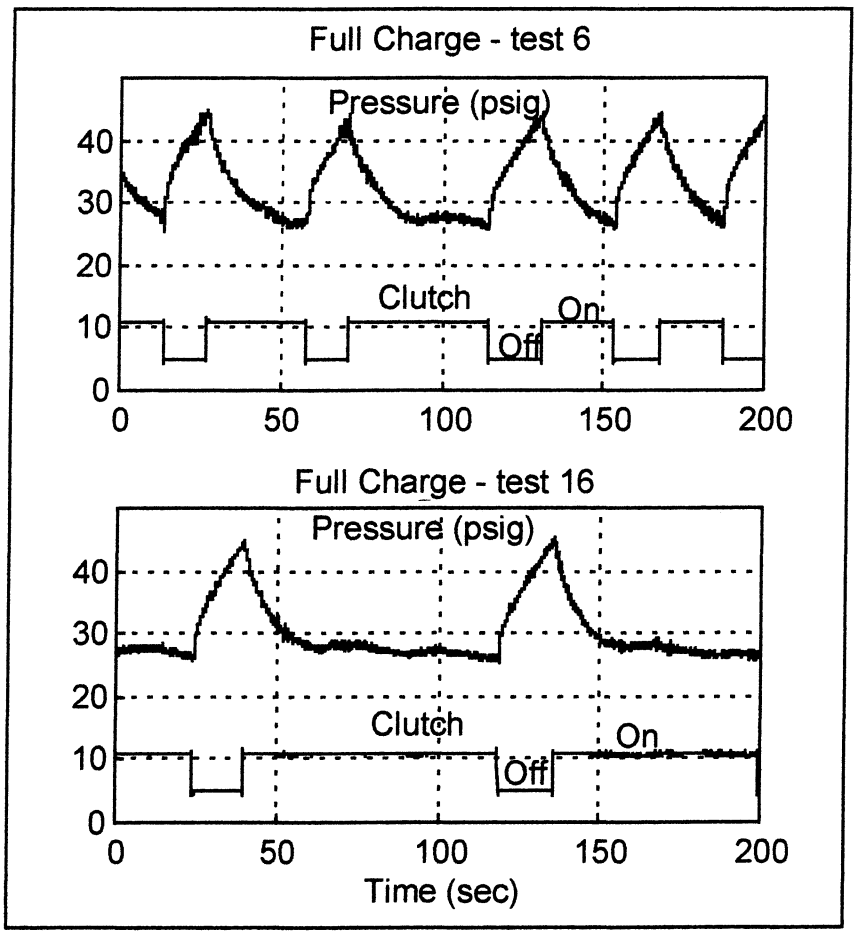

Figure 4.10 Examples of inconsistent cycle times. Note: Refrigerant pressure measured at the evaporator outlet.

The main and interaction effects for the total cycle time are given in Table 4.19. As expected from the data of Table 4.18, the refrigerant charge level has the largest

effect, and the condenser air inlet temperature and charge-condenser air temperature interaction are also quite large. However, due to the three tests that incurred long, inconsistent cycling mentioned above, the effects in Table 4.19 must be used with caution. The three long cycle times have a big impact on the magnitude of the effects, and the statistical analysis performed earlier would not give good results.

Table 4.19 Main and Interaction Effects for Cycle Time.

	Effect (sec)
Y (average)	40.45
x1	5.18
x2	14.80
x3	21.73
x4	-6.96
x1x2	3.10
x1x3	3.89
x1x4	4.51
x2x3	15.29
x2x4	-5.41
x3x4	-5.24
x1x2x3	3.20
x1x2x4	7.71
x1x3x4	4.86
x2x3x4	-2.24
x1x2x3x4	6.23

To get a better idea of how the refrigerant charge level affects the clutch cycle time of the system, we will compare the eight sets of tests where only the refrigerant charge is varied, Figure 4.11. For instance, in the 1-5 test group matched up in Figure 4.11, the refrigerant charge is the only parameter that is not the same. As you can see, a gap between the low and high charge curves is always maintained, but the 21.72 second difference found for the effect value is not a good representation. Over a wide range of conditions, the gap between the two curves is much smaller than what was expected.

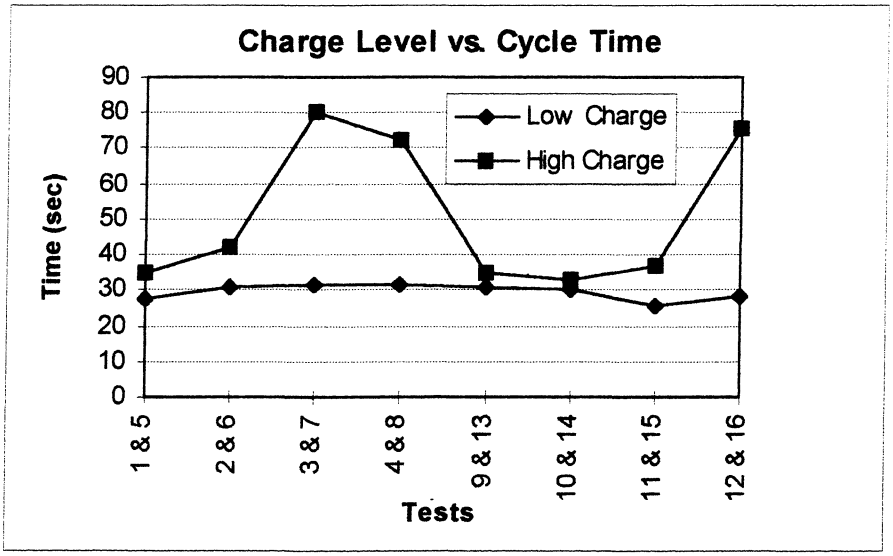

Figure 4.11 Low & full charge vs. cycle time while holding the other parameters constant. Other parameters vary from one group of tests to the next.

4.7 Discussion of Results.

Our results show that using the system clutch cycle time as a tool to detect charge loss may not be the best method. Every system parameter that was looked at has an impact on the cycle time; therefore, each one must either be accounted for or the system must be in an operating region where the effect of the parameter has been neutralized. The affect that humidity has on the system is also a concern because it is an unknown parameter. As shown in Figures 4.8 and 4.9, when the evaporator air inlet temperature is high, the difference in cycle time is significant, but the system only cycles at low values of humidity. If the vehicle is being operated in a region where the humidity is normally high, it may not ever see this particular operating range.

Although the method has its shortcomings, it is information that is already available. In other words, no sensors would have to be added. With today's climate control systems the system could be periodically driven to an operating regime of high evaporator air temperature and low humidity so that diagnostic checks could be performed. However, this may prove to be uncomfortable for the passengers. Once the system is in a desirable region, it would have to stay there for several minutes in order to

acquire several cycles to get a good average. Even in such a desirable region, because of the sensitivity of the cycle time to several system parameters, the cycle time method may not be able to meet our goal of detecting a small amount of refrigerant charge loss..

5. A LOOK AT EVAPORATOR REFRIGERANT OUTLET TEMPERATURE.

5.1 Introduction.

After taking a close look at the air conditioning system's clutch cycle time, I began looking for something else that could possibly indicate refrigerant charge loss. It appears that due to the large variability in the data and the sensitivity to humidity, it would be difficult to use the clutch cycle time to achieve our goal of detecting small amounts of charge loss. After looking at numerous plots of data, I noticed a trend in a particular variable that was being measured. This variable showed a considerable change when the refrigerant charge in the system was varied. The refrigerant temperature at the evaporator outlet, T_{ero}, was higher at the end of the "on" part of the cycle, i.e. at the instant that the clutch disengages, for the low charge case. Figure 5.1 shows this difference for a particular set of tests where only the charge has changed.

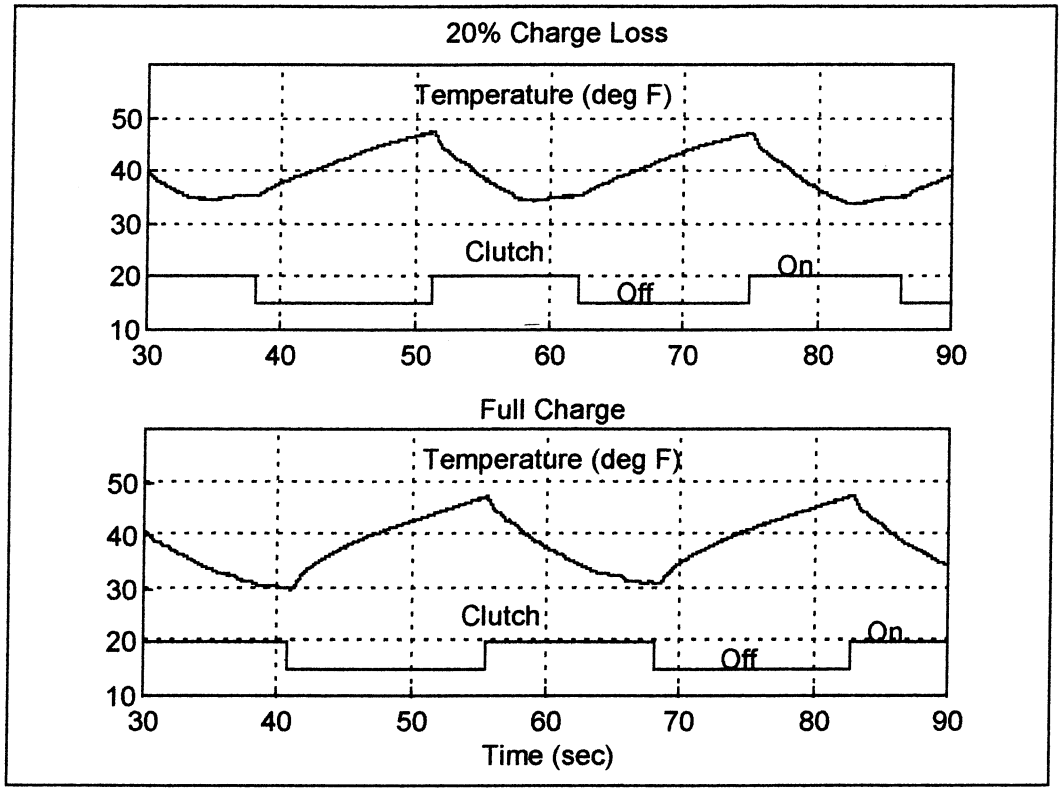

Figure 5.1 T_{ero} for a full charge test vs. a 20% low charge test.

Figure 5.1 shows a case where 20% of the charge has been lost, and there is already a significant increase in T_{ero} at the end of the cycle. From a physical perspective this rise in temperature made sense. For a given load, as the charge is reduced the quality of the refrigerant at the evaporator outlet increases until it reaches a saturated vapor state. If the charge continues to decrease, the refrigerant becomes superheated, and the outlet temperature begins to rise. Figure 5.2 shows a temperature versus entropy curve for R134a refrigerant with several different constant pressure lines included.

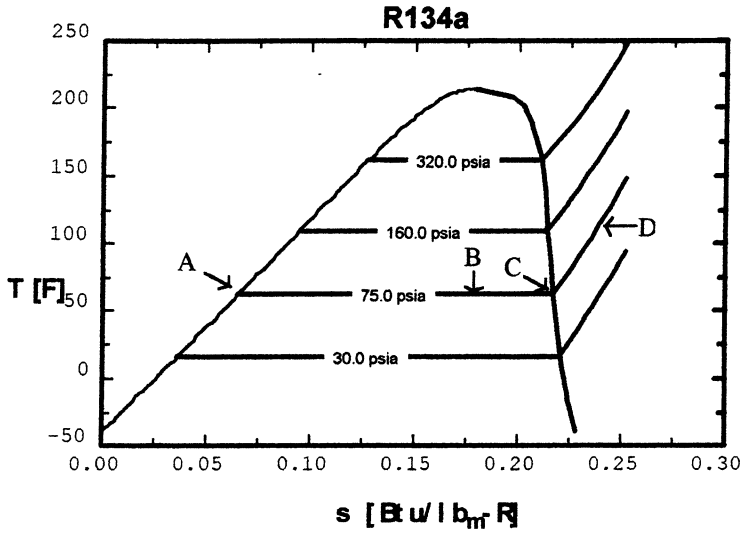

Figure 5.2 T-s diagram for R-134a [18].

The area under the dome in Figure 5.2 represents the region where the substance changes from the liquid phase to the vapor phase, and it is commonly referred to as the liquid-vapor saturation state. Although the refrigerant does experience a slight pressure drop as it passes through the evaporator, this small decrease is normally neglected. As is commonly known, for a given pressure, the temperature remains constant as the substance changes phase in the saturated region. The area to the right of the dome is the super-heated vapor region.

Let's assume that the refrigerant is entering the evaporator at 75 psia, which is indicated in Figure 5.2. The refrigerant has a very low or no quality, near point A. As heat is absorbed in the evaporator, the refrigerant begins to vaporize and move to

the right along the curve. Under normal conditions with a full charge, the refrigerant exits the evaporator with a high quality, around point B, but still in the saturated region. Therefore, the temperature has not changed. As refrigerant charge is lost, the quality becomes greater until it becomes a saturated vapor, point C. If charge loss continues, the refrigerant is pushed into the superheated region, point D, where the temperature begins to rapidly increase. But, how will this temperature react to changes in the other system parameters? For instance, will an increase in condenser air inlet temperature also cause an increase in T_{ero} by pushing it into the superheated region? To determine the impact of the various parameters on T_{ero}, we will return to the two-level full factorial design matrices.

5.2 Using 2^5 Design Matrix to Examine T_{ero}.

Using T_{ero} as a diagnostic tool seemed to have potential; so, I returned to the data from the 2^5 design matrix discussed in section 4.2 in order to study how all of the system parameters affect T_{ero}. The same 32 tests that were used to collect the cycle times of Table 4.4 where used to collect T_{ero}. The average value of T_{ero} at the end of the cycle for each test is given in Table 5.1 below. Recall that the parameter values for these tests are given in Table 4.3 of section 4.2..

Following the example set in section 4.2, the data will now be broken down and averaged over the (+) and (-) groups for each of the five parameters of Table 4.1 in order to better see the effect of each parameter on T_{ero}. The results are given in Table 5.2 along with the standard deviations. The data of Table 5.2 indicates that the condenser air flow rate and condenser air inlet temperature have practically no effect on T_{ero}, and the compressor speed has only a small effect. An increase in the evaporator air inlet temperature causes a small increase in T_{ero}, but the refrigerant charge level provides the most significant impact on T_{ero}. It is also interesting to note that the standard deviations of the (+) and (-) groups for refrigerant charge are quite small. This is an indication that the other parameters, as well as the interactions between the various parameters, are quite small.

Table 5.1 T_{ero} for 2^5 design Matrix.

	Parameters					T_{ero}	Std Dev
Test	1	2	3	4	5	(°F)	(°F)
1	-	-	-	-	-	34.11	0.57
2	+	-	-	-	-	33.97	1.81
3	-	+	-	-	-	31.79	0.90
4	+	+	-	-	-	34.18	0.56
5	-	-	+	-	-	36.61	1.38
6	+	-	+	-	-	37.35	0.71
7	-	+	+	-	-	34.08	0.49
8	+	+	+	-	-	36.68	2.48
9	-	-	-	+	-	30.58	1.26
10	+	-	-	+	-	29.60	0.36
11	-	+	-	+	-	30.71	0.96
12	+	+	-	+	-	29.56	0.31
13	-	-	+	+	-	31.17	1.32
14	+	-	+	+	-	31.77	1.83
15	-	+	+	+	-	30.65	2.13
16	+	+	+	+	-	31.29	1.88
17	-	-	-	-	+	33.01	2.14
18	+	-	-	-	+	30.68	0.38
19	-	+	-	-	+	33.34	0.85
20	+	+	-	-	+	33.52	1.00
21	-	-	+	-	+	34.60	1.63
22	+	-	+	-	+	35.29	0.82
23	-	+	+	-	+	35.52	1.40
24	+	+	+	-	+	33.86	0.44
25	-	-	-	+	+	30.81	1.63
26	+	-	-	+	+	30.69	1.23
27	-	+	-	+	+	31.48	0.81
28	+	+	-	+	+	30.82	1.27
29	-	-	+	+	+	30.27	1.26
30	+	-	+	+	+	30.20	1.06
31	-	+	+	+	+	30.37	0.66
32	+	+	+	+	+	30.08	0.60
			Average			32.46	2.26

Table 5.2 Analysis of Parameter Effects on T_{ero}.

	Average (°F)	Std Dev (°F)
All Tests	32.46	2.26
Cond Air Flow (+)	32.47	2.53
Cond Air Flow (-)	32.44	2.04
Cond Air Temp (+)	32.37	2.11
Cond Air Temp (-)	32.54	2.47
Evap Air Temp (+)	33.11	2.65
Evap Air Temp (-)	31.80	1.62
Ref. Charge (+)	30.63	0.62
Ref. Charge (-)	34.29	1.75
Comp Speed (+)	32.16	1.95
Comp Speed (-)	32.75	2.56

5.3 Analysis of 2^5 Design Matrix.

The next step is to look at the main and interaction effects, and they should support the data from Table 5.2. As was the case with the cycle times earlier, it is assumed that only the four and five-factor interactions are equal to zero. Thus, the main, two, and three-factor interactions will be considered for inclusion in the model for T_{ero}, and they are given in Table 5.3.

From the effects listed in Table 5.3, the main effect of refrigerant charge is almost three times as large as the next largest effect, and this is a promising result. Much more analysis is needed, especially the effect of humidity on T_{ero}, but the preliminary numbers look promising. Once again, the higher order interactions, listed in Table 5.4, are assumed to be zero; therefore, any value that they have is assumed to be due to variability in the data. The small values of the higher order interactions in Table 5.4 indicate that the variability is small, but a quantitative approach is needed.

Table 5.3 Main, Two, and Three Factor Interactions for T_{ero}.

	Effect (°F)
Y (average)	32.46
x1	0.03
x2	-0.18
x3	1.31
x4	-3.66
x5	-0.60
x1x2	0.23
x1x3	0.38
x1x4	-0.28
x1x5	-0.56
x2x3	-0.42
x2x4	0.16
x2x5	0.60
x3x4	-1.11
x3x5	-0.58
x4x5	0.52
x1x2x3	-0.31
x1x2x4	-0.34
x1x2x5	-0.30
x1x3x4	0.10
x1x3x5	-0.18
x1x4x5	0.53
x2x3x4	0.18
x2x3x5	-0.14
x2x4x5	-0.39
x3x4x5	-0.34

Table 5.4 Higher Order Interaction Effects for T_{ero}.

Interaction	Effect (°F)
x1x2x3x4	0.38
x1x2x3x5	-0.25
x1x2x4x5	0.22
x1x3x4x5	-0.19
x2x3x4x5	0.18
x1x2x3x4x5	0.27

The effects of Table 5.4 result in the following value for the variance of the data.

$$s^2_{effect} = \sum_{\substack{higher-order \\ interactions}} \frac{(E_i)^2}{6} = 0.066$$

The estimated sample standard deviation , s_{effect}, is 0.257. For consistency we will once again use the sample standard deviation to build a 95% confidence interval for the effects of Table 5.3. From chapter 4,

$t_{32,0.975} = 2.038$. This results in:

$E_i \pm (2.038)*(0.257)$

$E_i \pm 0.52$

The confidence interval of 0.52 for T_{ero} is much smaller than the 1.57 value that was computed in section 4.2.2 for the cycle time. To use a more common phrase, the T_{ero} data has much less "noise" in it. Table 5.5 lists the effects of Table 5.3 that we are 95% confident have a significant impact on T_{ero}.

Table 5.5 Significant Effects for T_{ero}-95% Confidence.

	Effect (°F)
Y (average)	32.46
x3	1.31
x4	-3.66
x5	-0.60
x1x5	-0.56
x2x5	0.60
x3x4	-1.11
x3x5	-0.58
x4x5	0.52
x1x4x5	0.53

Unlike the 95% confidence interval for the clutch cycle time, we are left with a large number of terms in the model for T_{ero}. The effects that we have determined to be significant result in the following equation for T_{ero}.

$$T_{ero} = Y + b_3*x3 + b_4*x4 + b_5*x5 + b_{15}*x1*x5 + b_{25}*x2*x5 + b_{34}*x3*x4 + b_{35}*x3*x5 + b_{45}*x4*x5 + b_{145}*x1*x4*x5$$

$$T_{ero} = 32.46 + 0.66*x3 - 1.83*x4 - 0.30*x5 - 0.28*x1*x5 + 0.30*x2*x5 - 0.56*x3*x4 - 0.29*x3*x5 + 0.26*x4*x5 + 0.27*x1*x4*x5$$

Now that the model has been formed, the fit of the model to the original data can be checked.

Table 5.6 Check of T_{ero} Model-95% Confidence.

Test	T_{ero} (°F) Measured	Predicted	% Error
1	34.11	33.10	-2.95
2	33.97	34.19	0.65
3	31.79	32.50	2.23
4	34.18	33.59	-1.74
5	36.61	36.10	-1.39
6	37.35	37.19	-0.42
7	34.08	35.50	4.18
8	36.68	36.59	-0.24
9	30.58	30.56	-0.05
10	29.60	30.60	3.38
11	30.71	29.96	-2.43
12	29.56	29.99	1.47
13	31.17	31.34	0.53
14	31.77	31.37	-1.25
15	30.65	30.74	0.29
16	31.29	30.77	-1.68
17	33.01	33.05	0.12
18	30.68	31.96	4.16
19	33.34	33.65	0.93
20	33.52	32.56	-2.85
21	34.60	34.89	0.84
22	35.29	33.80	-4.21
23	35.52	35.49	-0.06
24	33.86	34.40	1.61
25	30.81	30.50	-1.03
26	30.69	30.47	-0.73
27	31.48	31.10	-1.20
28	30.82	31.07	0.81
29	30.27	30.11	-0.53
30	30.20	30.08	-0.40
31	30.37	30.71	1.14
32	30.08	30.68	2.02

Table 5.6 shows that all of the predicted values are within 5% error with the largest being test 22 at -4.21, and this is much smaller than the maximum of 15.05 for the

clutch cycling data. Using the equation for the average percent absolute deviation described in section 4.3 results in,

APD = 1.48

as compared to an APD of 5.34 for the cycle time. The percent deviation of the equation for T_{ero} is approximately one-fourth that of the equation for the cycle time. The model for T_{ero} results in a much improved fit of the data as compared to the model for the cycle time, CT, in section 4.2, based on a 95% confidence interval.

Following the example set in chapter 4, we will now look at the effect on the equation for T_{ero} when a more relaxed 80% confidence interval is used. Using the data from chapter 4,

$t_{32,0.90} = 1.309$. This results in:

$E_i \pm (1.309)*(0.257)$, or $E_i \pm 0.34$

The confidence interval of 0.34 for T_{ero} is again much smaller than the 1.01 that was computed in chapter 4 for the cycle time. Table 5.7 lists the effects of Table 5.3 that we are 80% confident have a significant impact on T_{ero}.

Table 5.7 Significant Effects for T_{ero}-80% Confidence.

	Effect (°F)
Y (average)	32.46
x3	1.31
x4	-3.66
x5	-0.60
x1x3	0.38
x1x5	-0.56
x2x3	-0.42
x2x5	0.60
x3x4	-1.11
x3x5	-0.58
x4x5	0.52
x1x2x4	-0.34
x1x4x5	0.53
x2x4x5	-0.39
x3x4x5	-0.34

We are now left with fifteen significant terms in the model for T_{ero} compared to ten terms for the case using a 95% confidence interval. Recall that for an 80% confidence interval of the cycle time, only eight terms were included. The smaller variance for T_{ero} should result in a more accurate model. The significant effects of Table 5.7 result in the following equation for T_{ero}.

$$T_{ero} = Y + b_3*x3 + b_4*x4 + b_5*x5 + b_{13}*x1*x3 + b_{15}*x1*x5 + b_{23}*x2*x3 + b_{25}*x2*x5 + b_{34}*x3*x4 + b_{35}*x3*x5 + b_{45}*x4*x5 + b_{124}*x1*x2*x4 + b_{145}*x1*x4*x5 + b_{245}*x2*x4*x5 + b_{345}*x3*x4*x5$$

$$T_{ero} = 32.46 + 0.66*x3 - 1.83*x4 - 0.30*x5 + 0.19*x1*x3 - 0.28*x1*x5 - 0.21*x2*x3 + 0.30*x2*x5 - 0.56*x3*x4 - 0.29*x3*x5 + 0.26*x4*x5 - 0.17*x1*x2*x4 + 0.27*x1*x4*x5 - 0.20*x2*x4*x5 - 0.17*x3*x4*x5$$

This new equation will now be used to estimate the expected temperatures, and the values will again be compared to the experimental data. The resulting values and errors are given in Table 5.8.

The model for T_{ero} is now in very good agreement with the experimental data of Table 5.1, and the largest error is only 3.64%. The resulting calculations for the APD give,

APD = 1.10

This is not much of an improvement over the model for the 95% confidence interval which had an APD of 1.48, but that is not necessarily bad. The equation fit so well for the case of a 95% confidence interval that there is not much room for improvement. Even though only fifteen terms, out of a possible thirty-two, are included in the model, it results in an extremely good fit of the original experimental data. This is another strong indication that there is very little variability in the temperature measurement taken at the end of the compressor cycle.

Table 5.8 Check of T_{ero} Model-80% Confidence.

Test	T_{ero} (°F)		% Error
	Measured	Predicted	
1	34.11	33.61	-1.44
2	33.97	33.98	0.05
3	31.79	32.70	2.86
4	34.18	33.75	-1.27
5	36.61	36.32	-0.79
6	37.35	37.45	0.27
7	34.08	34.57	1.44
8	36.68	36.37	-0.82
9	30.58	30.01	-1.86
10	29.60	30.00	1.37
11	30.71	30.56	-0.49
12	29.56	29.87	1.06
13	31.17	31.16	-0.04
14	31.77	31.91	0.44
15	30.65	30.87	0.73
16	31.29	30.94	-1.12
17	33.01	32.83	-0.53
18	30.68	31.03	1.12
19	33.34	33.91	1.71
20	33.52	32.78	-2.20
21	34.60	35.05	1.30
22	35.29	34.00	-3.64
23	35.52	35.29	-0.64
24	33.86	34.92	3.13
25	30.81	30.67	-0.46
26	30.69	30.60	-0.29
27	31.48	31.64	0.51
28	30.82	30.89	0.23
29	30.27	29.99	-0.93
30	30.20	30.68	1.58
31	30.37	30.12	-0.81
32	30.08	30.13	0.18

5.4 T_{ero} vs. Refrigerant Charge Level.

To get a better idea of how T_{ero} would react as the charge level continues to decrease, I looked back at the tests of section 4.4. The test conditions are listed in Table 5.9 (note: this data is from the same tests of section 4.4 used to collect cycle time data).

After conducting the tests and analyzing the data, the following values and standard deviations for T_{ero} (averaged over a number of cycles), listed in Table 5.10, were computed.

Table 5.9 Test Conditions for T_{ero} vs. Charge Level Tests.

Test	Cond Air Flow (cfm)	Cond Air Temp (°F)	Evap Air Temp (°F)	Compressor Speed (rpm)	Humidity (%RH)
A	1675	100	65	1700	20
B	1850	110	70	1700	20

Table 5.10 T_{ero} vs. Refrigerant Charge Level.

Ref. Charge	% of	Test A (°F)		Test B (°F)	
(lbs)	Optimum	T_{ero}	Std Dev	T_{ero}	Std Dev
2.05	70	35.61	1.28	39.61	0.68
2.35	80	35.66	0.35	37.42	0.59
2.65	90	32.46	1.19	32.45	0.96
2.95	100	30.09	0.57	30.28	0.23
3.25	110	28.82	0.22	29.58	0.49

It is obvious from the data in Table 5.10 that as the refrigerant charge is lost, the temperature at the evaporator outlet continues to increase. Figure 5.3 shows the raw data for three different charge levels of the Test B conditions. You can see how the temperature reaches a minimum and begins to rise into the superheated region for the low charge tests. The data listed in Table 5.10 is plotted in Figure 5.4 for better visualization purposes.

Figure 5.4 clearly shows the gradual increase in T_{ero} as the charge is reduced. The difference in test conditions does have a slight effect, but the two curves still follow the same trend. For the "A" test conditions, T_{ero} experiences no increase between 80 and 70% charge, but this is not a concern. It is still significantly greater than T_{ero} for the optimum charge level.

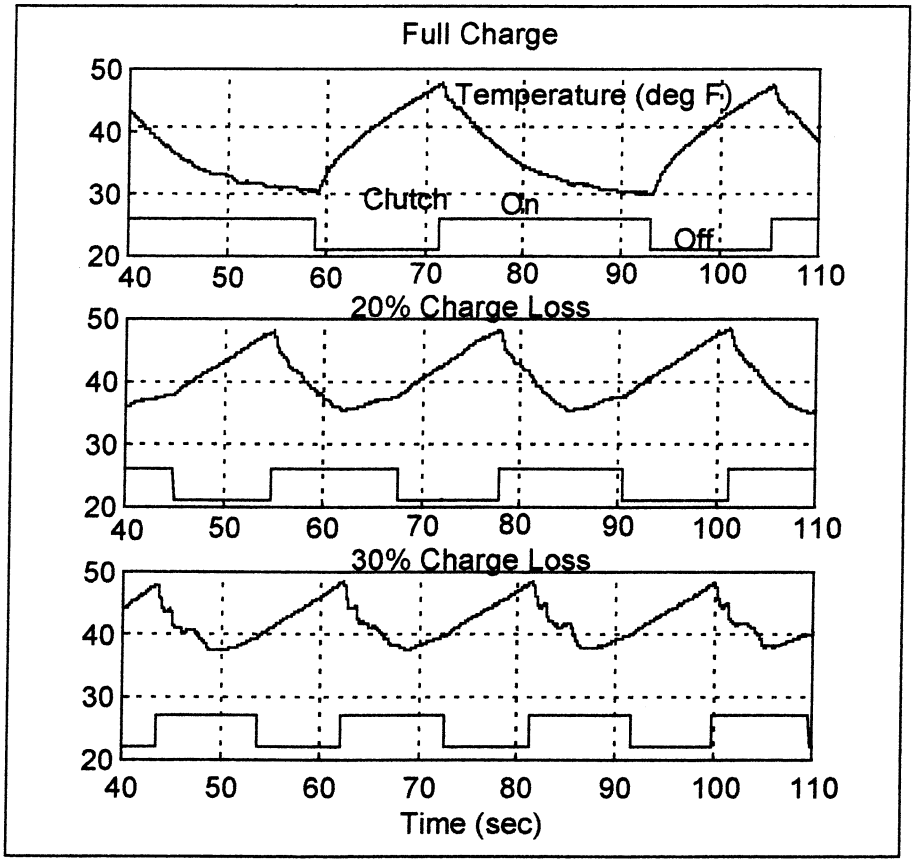

Figure 5.3 Comparison of T_{ero} as refrigerant charge decreases.

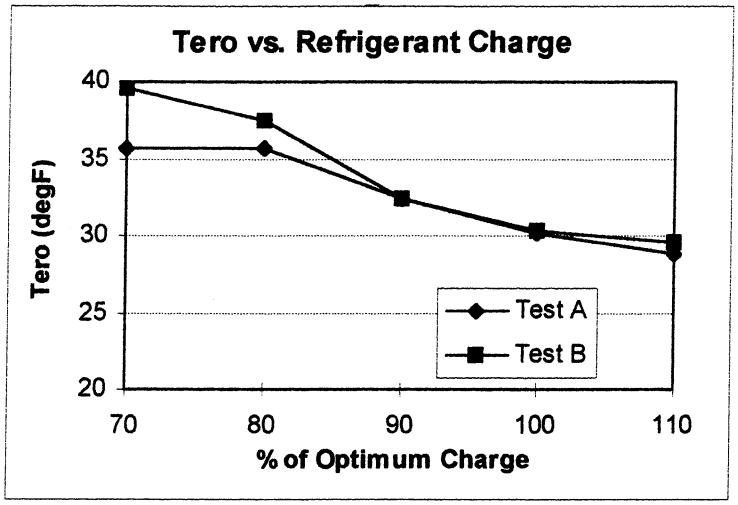

Figure 5.4 Comparison of T_{ero} vs. refrigerant charge.

5.5 Effect of Humidity on T_{ero}.

From our analysis so far, the refrigerant charge level has a significant impact on T_{ero}, but what impact does humidity have on T_{ero}? As we saw in section 4.5, the humidity had a significant impact on the clutch cycle time, and it adds a lot of complexity to the possibility of using the clutch cycle time to detect charge loss. To investigate the effect of humidity on T_{ero}, I analyzed the same data that was obtained to observe the effect of humidity on the clutch cycle time. As a reminder, the test conditions (Table 4.14) are listed here in Table 5.11.

Table 5.11 Test Conditions for T_{ero} vs. Humidity Experiments.

Test	Cond Air Flow (cfm)	Cond Air Temp (°F)	Evap Air Temp (°F)	Compressor Speed (rpm)	Refrigerant Charge (lbs)
A1	1675	100	65	1950	2.35
A2	1675	100	65	1950	2.95
B1	1675	100	70	1950	2.35
B2	1675	100	70	1950	2.95
C1	1675	100	80	1950	2.35
C2	1675	100	80	1950	2.95
D1	1675	100	85	1950	2.35
D2	1675	100	85	1950	2.95

A "1" in Table 5.11 signifies a 20% charge loss, and a "2" signifies a full charge. Table 5.12 lists the results for the tests of Table 5.11. An average of 8 to 12 cycles were used in each test to get an average value for T_{ero}, and one important thing to point out is the low standard deviations that resulted. The largest standard deviation for all of the tests is 2.57 °F. Figure 5.5 shows how stable T_{ero} is even under extreme conditions. The data looks different for each cycle, but for the top plot the average for T_{ero} is 58.03 °F with a standard deviation of only 0.84. Recall that for this same test the cycle time is 32.01 seconds with a standard deviation of 16.31. The lower curve has a cycle time of 69.09 seconds with a standard deviation of 21.17 and a T_{ero} of 31.88 °F and 2.22 standard deviation..

Table 5.12 T_{ero} for Various Humidity Levels.

Experiment	% Relative Humidity			
	20		40	
	T_{ero} (°F)	Std (°F)	T_{ero} (°F)	Std (°F)
A1	34.27	1.12	36.75	0.57
A2	29.72	0.56	28.36	1.10
B1	37.68	0.71	41.51	0.82
B2	31.78	2.08	29.08	1.02
C1	42.90	1.04	52.72	0.52
C2	35.03	2.57	no cycle	---
D1	47.41	1.85	61.29	2.05
D2	31.88	2.22	no cycle	---
	% Relative Humidity			
Experiment	60		80	
	T_{ero} (°F)	Std (°F)	T_{ero} (°F)	Std (°F)
A1	42.06	0.67	48.73	1.11
A2	29.93	0.28	no cycle	---
B1	49.65	0.83	58.03	0.84
B2	no cycle	---	no cycle	---
C1	no cycle	---	no cycle	---
C2	no cycle	---	no cycle	---
D1	no cycle	---	no cycle	---
D2	no cycle	---	no cycle	---

The data of Table 5.12 is not very easy to compare; so, the graphs of Figures 5.6-5.9 will make the results easier to visualize. Like the clutch cycle time data in section 4.5, the graphs do not include data for the higher humidity values because the system did not cycle. Obviously, there is still a measurable temperature at the evaporator outlet, but if the system is not cycling, the pressure of the refrigerant is not known. If the pressure is unknown, no valid assumptions can be made about T_{ero}. The system is designed to have a small amount of liquid at the exit of the evaporator (i.e. the R-134a is in the two-phase region), and at the end of the cycle the pressure is known due to the low pressure cutoff switch. Thus, the temperature at this point should be at or near the saturation temperature for R-134a.

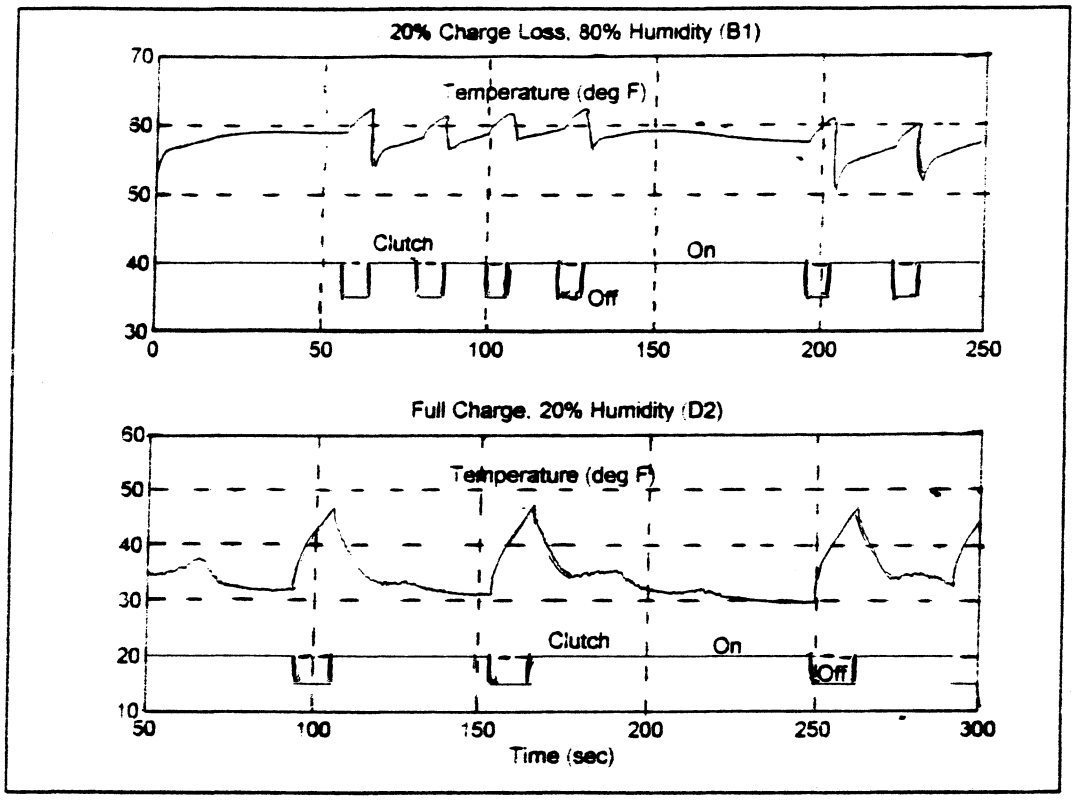

Figure 5.5 Examples of small deviations of T_{ero} under extreme conditions.

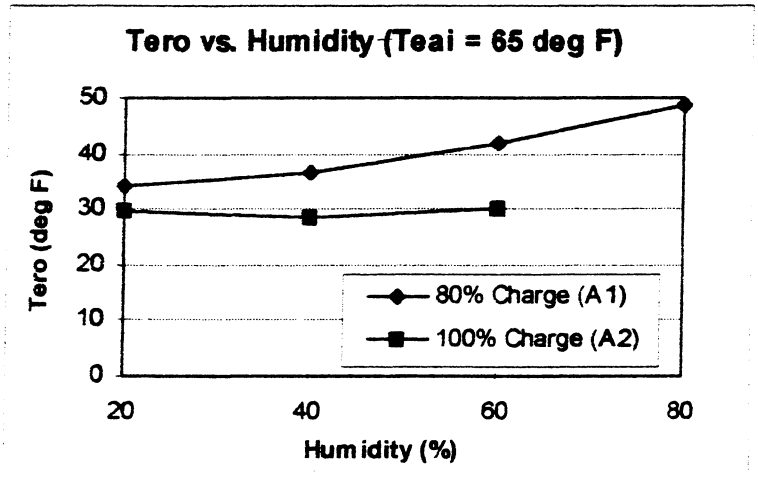

Figure 5.6 T_{ero} vs. Humidity for T_{eai} = 65 °F. Note: Missing data points indicate that the system did not cycle.

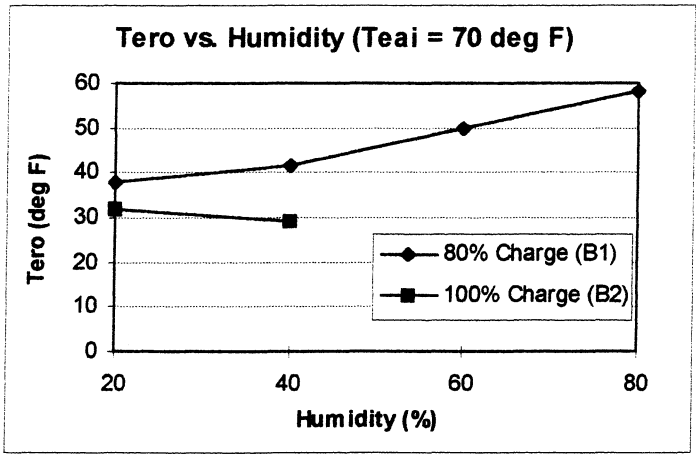

Figure 5.7 T_{ero} vs. Humidity for T_{eai} = 70 °F.

The plots of Figures 5.6 and 5.7 show practically no effect of humidity on the evaporator refrigerant outlet temperature for a full charge. No matter what the humidity is, there is a region that separates the two curves. This region is bounded by the lowest temperature for the low charge tests and the highest temperature for the full charge tests. For the tests that are 20% low in charge, T_{ero} does gradually increase as the humidity increases, but that is not a concern. This increase of T_{ero} makes it that much easier to identify a loss of charge by widening the gap between the full and low charge tests.

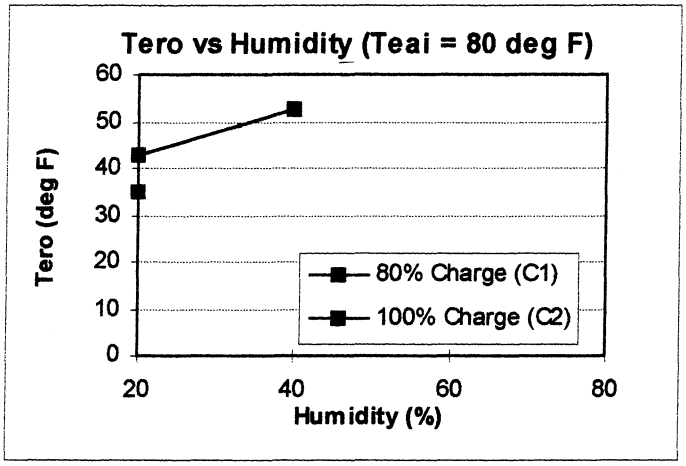

Figure 5.8 T_{ero} vs. Humidity for T_{eai} = 80 °F.

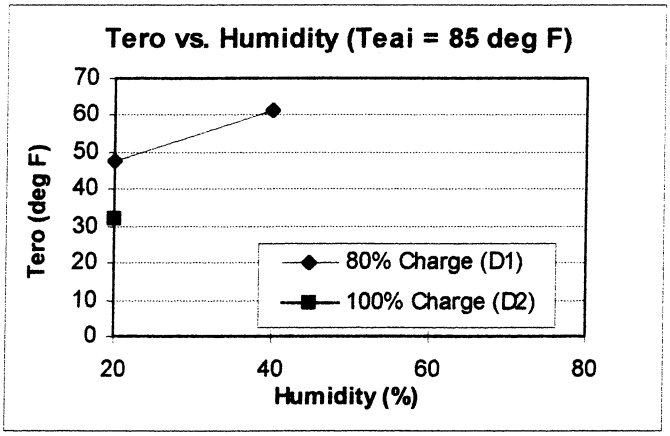

Figure 5.9 T_{ero} vs. Humidity for T_{eai} = 85 °F.

Figures 5.8 and 5.9 once again show a clear difference in T_{ero} between the full charge and 20% low charge tests for higher evaporator air inlet temperatures. As was the case with the lower evaporator air temperatures of Figures 5.6 and 5.7, the only humidity effect is an increase in T_{ero} for the low charge tests. Over a wide range of vehicle cabin temperatures, the cabin humidity has an insignificant impact on the evaporator refrigerant outlet temperature.

5.6 2^4 Design Matrix Under High Load Conditions.

In sections 5.2 and 5.3 we saw that a loss of charge causes an increase in T_{ero} over the range of parameters tested. However, since the evaporator air inlet temperatures that were used are on the low side of the comfortable region, it is wise to take a look at how the refrigerant charge, as well as other parameters, affect T_{ero} at higher evaporator air temperatures. The data will be extracted from the tests of section 4.6 that were used to gather cycle time data. Recall that the evaporator conditions are: 80 °F air inlet temperature and 220 cfm air flow, and the other parameter settings are given in Table 5.13. Note that the low value of refrigerant charge represents a 20% loss of charge.

Table 5.13 Parameter Values for 2^4 Experimental Design Matrix.

Tag	Parameter		High(+)	Low(-)
1	Condenser Air Flow	(cfm)	1850	1675
2	Condenser Air Temp	(°F)	110	100
3	Refrigerant Charge	(lbm)	2.95	2.35
4	Compressor Speed	(rpm)	1950	1700

As usual, T_{ero} was averaged over a number of cycles for each set of test conditions, and the resulting temperatures, along with the standard deviations, are listed in Table 5.14. Since these tests were conducted with 20% charge loss instead of 10% and under higher loads, the low charge tests were expected to be well into the superheated region. This hypothesis was proven correct since all of the low charge tests have average T_{ero} values of over 40 °F.

Table 5.14 2^4 Test Matrix and T_{ero} Values.

Test	Parameter				T_{ero}	Std Dev
	1	2	3	4	(°F)	(°F)
1	-	-	-	-	41.52	1.05
2	+	-	-	-	41.71	0.77
3	-	+	-	-	44.09	0.48
4	+	+	-	-	43.64	0.60
5	-	-	+	-	33.51	0.36
6	+	-	+	-	34.00	2.56
7	-	+	+	-	30.62	0.86
8	+	+	+	-	30.75	1.21
9	-	-	-	+	41.47	0.60
10	+	-	-	+	41.31	0.64
11	-	+	-	+	42.04	0.61
12	+	+	-	+	42.79	1.22
13	-	-	+	+	32.66	0.96
14	+	-	+	+	32.18	0.86
15	-	+	+	+	33.82	1.97
16	+	+	+	+	30.43	0.95
			Average:		37.28	0.98

As before, Table 5.15 gives a breakdown of the (+) and (-) tests for each parameter that was varied. The refrigerant charge level seems to be the only parameter that had any significant effect at all on T_{ero}, and the standard deviations for the low and high refrigerant charge levels are quite small. This means that the change in T_{ero} due to a change in charge level remains fairly constant as the other parameters are varied. The main and interaction effects for the tests shown in Table 5.14 are given in Table 5.16.

Table 5.15 Analysis of Parameter Effects on T_{ero}.

	Average(°F)	Std Dev(°F)
All Tests	37.28	5.35
Cond Air Flow (+)	37.10	5.77
Cond Air Flow (-)	37.47	5.29
Cond Air Temp (+)	37.27	6.39
Cond Air Temp (-)	37.30	4.53
Ref. Charge (+)	32.25	1.49
Ref. Charge (-)	42.32	1.06
Comp Speed (+)	37.09	5.25
Comp Speed (-)	37.48	5.81

Table 5.16 Main and Interaction Effects for T_{ero} Under High Loads.

	Effect (sec)
Y (average)	37.28
x1	-0.37
x2	-0.02
x3	-10.08
x4	-0.39
x1x2	-0.38
x1x3	-0.45
x1x4	-0.46
x2x3	-1.66
x2x4	0.39
x3x4	0.45
x1x2x3	-0.44
x1x2x4	-0.13
x1x3x4	-0.67
x2x3x4	1.00
x1x2x3x4	-0.51

The magnitude of the refrigerant charge level effect on T_{ero} is 10.08. This effect is only half as large as the effect on the cycle time, but in Table 5.16 no other effect even comes close to the magnitude of the refrigerant charge effect. The refrigerant charge effect is six times larger than the second largest effect. Figure 5.10 gives a comparison of the eight pairs of tests where only the refrigerant charge is varied. It is clearly evident that the refrigerant charge level has a significant impact on T_{ero}. No matter what value

the other parameters are set at, a continuous gap of 7.31 °F exists between the full charge and low charge lines.

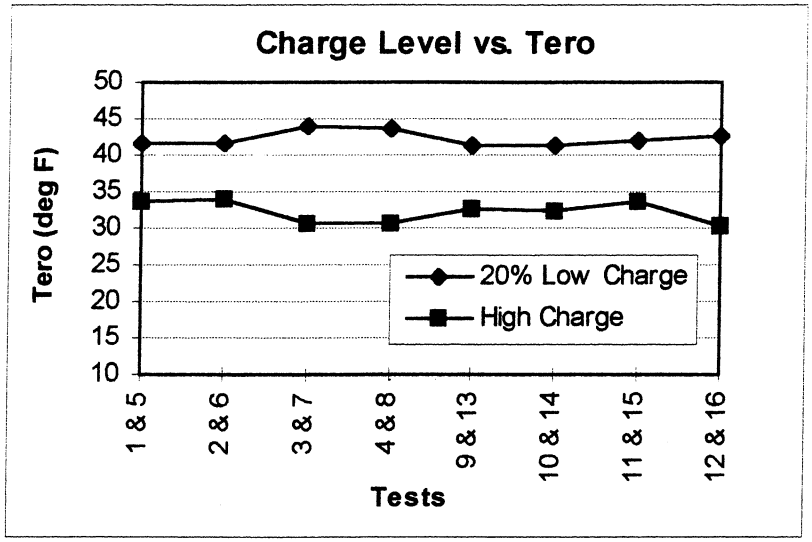

Figure 5.10 T_{ero} vs. charge level under high load conditions. Each set (ex. 1 & 5) represent a change in charge only. Other parameters vary from one set to the next.

5.7 Discussion of Results for T_{ero}.

The results of the above tests and analysis is very promising. There is a definite link between the refrigerant charge level and the evaporator refrigerant outlet temperature, and this temperature is not very sensitive to the other dynamic system parameters. The evaporator air inlet temperature has a small effect, but it is already known on many vehicles making it easy to account for its effect. The humidity only affects T_{ero} after significant charge loss has occurred, but its effect only makes it easier to recognize the loss of refrigerant charge by increasing T_{ero} even more, widening the gap between the full and low charge tests..

Studies have shown that the amount of oil circulating in the system drops once the refrigerant temperature at the evaporator outlet becomes superheated. Tests conducted by [19] showed that the amount of oil remaining in the evaporator increases, thus decreasing the amount of circulating oil, once the evaporator outlet becomes superheated,

> "During evaporation, pressure had little effect on the oil in the test section, but introducing an exit temperature above that of saturated pure refrigerant increased the quantity of oil significantly."

The analysis of T_{ero} revealed that the measurement is quite reliable, and there is very little variability in the data. The only obvious drawback to using T_{ero} as a diagnostic tool to detect refrigerant charge loss is the fact that it would require the addition of a sensor. While temperature measurements are quite inexpensive, for an automotive company, adding a sensor to several million vehicles a year can be a significant expense.

6. RESTRICTED CONDENSER AIR FLOW.

6.1 Introduction.

Up to this point, most of the discussion has focused on refrigerant charge loss and possible methods for detecting the loss of charge. While charge loss is the most common problem and raises the most concern, it is not the only possible system fault that can occur. Another possible A/C system fault is a fouled, partially clogged or blocked, condenser. This reduces the air flow across the condenser coils; therefore, the amount of heat removed from the system is reduced. Most vehicles are driven on paved roads in urban areas, and it is unlikely that the condenser will become fouled in such an environment. However, many four-wheel drive trucks, farm machines, and mining equipment experience harsh environments that can foul a condenser coil. As discussed earlier, a big concern in fault diagnosis is false positives; therefore, the immediate question is what impact does a fouled condenser have on the system's clutch cycle time or evaporator refrigerant outlet temperature? It is quite possible that such a fault could produce a similar change in the variables that have been studied so far, and this would be an obstacle for the two charge loss detection methods being considered. While detecting charge loss is highly desirable, any significant amount of false positives would be a big disadvantage. For example, we have shown that a reduction in refrigerant charge increases T_{ero}. Suppose that a fouled condenser also increases T_{ero}, and that your truck condenser has become fouled by driving through the fields on your farm. The truck senses the rise in T_{ero} and tells you that the A/C system is low on charge. You get the local mechanic to recharge the system. Money and time have been wasted unnecessarily, and the problem is still there. Reliability is very important in the automotive industry, as well as many other fields. Another concern is the interaction effect of a fouled condenser and low charge on the clutch cycle time and T_{ero}. For example, suppose that charge reduction increases T_{ero}, but a fouled condenser reduces T_{ero}. Your truck's condenser is gradually becoming fouled, and at the same time the system is losing charge. The effects of the two faults on T_{ero} could counteract one another, and the charge loss would go undetected.

6.2 Effect of a Fouled Condenser on a Fully Charged System.

It was decided that only a small set of tests would be needed in order to see what kind of effect a restricted condenser would have on the clutch cycle time and evaporator refrigerant outlet temperature. Instead of conducting a two-level factorial design matrix, which would require a larger number of tests, all of the other parameters (besides condenser air flow) were held constant in all but one of the tests. A 2^k design matrix works well if a detailed statistical analysis is desirable, but a smaller number of tests should be sufficient when you are only trying to capture a trend in the data. A total of five tests were conducted, and the parameter values are given in Table 6.1. Note that test five has higher evaporator and condenser air inlet temperatures in order to acquire a data set under high system load conditions.

Table 6.1 Parameter Values for Restricted Condenser Tests.

Test	Cond. Air Flow (cfm)	Cond. Air Temp (°F)	Evap. Air Temp (°F)	Ref. Charge (lbs)	Compressor Speed (rpm)
1	1700	100	70	2.95	1950
2	1450	100	70	2.95	1950
3	1200	100	70	2.95	1950
4	1000	100	70	2.95	1950
5	1200	110	80	2.95	1950

6.2.1 Effect on Clutch Cycle Time.

After the tests were conducted, the data produced the cycle times shown in Table 6.2. Note that the on, off, and total cycle times are given. Table 6.2 indicates that the total clutch cycle time is inversely proportional to the condenser air flow. As the air flow decreases, the system cycle time increases, and most of the change occurs between 1450 and 1200 cfm. Figure 6.1 clearly shows the effect of a restricted condenser on the total cycle time.

Table 6.2 Cycle Times for Restricted Condenser Tests.

Test	On (sec)		Off (sec)		Total (sec)	
	Cycle	Std Dev	Cycle	Std Dev	Cycle	Std Dev
1	16.41	0.56	14.57	0.97	30.98	1.35
2	15.90	2.73	14.11	1.07	30.01	3.69
3	27.27	5.40	14.28	6.36	41.55	11.23
4	27.36	7.29	15.78	1.44	43.14	6.85
5	No cycle	---	No cycle	---	No cycle	---

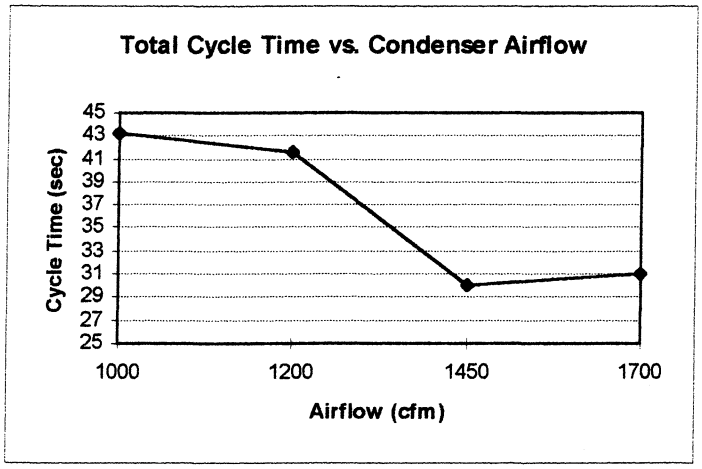

Figure 6.1 Total cycle time vs. condenser air flow.

The test at 1700 cfm is just above idle conditions which would be the lowest air flow that the vehicle would see; therefore, 1450 cfm represents a 14.7% reduction in air flow. At this point the cycle time has not been affected. 1200 cfm represents a 29.4% reduction in air flow, and beyond this point the change in the cycle time is small. So, between 15% and 30% reduction in air flow, the cycle time jumps by almost 40%. Without taking more data at smaller increments of air flow, the exact range over which the change occurs is unclear; therefore, according to our tests the condenser air flow would need to be accounted for after a 15% reduction has occurred. If it is not accounted for, it could offset the effect that refrigerant charge loss would have on the system, and the charge loss would go undetected. Small changes in condenser air flow have been

shown to be insignificant in section 4.2, but this parameter, as well as the refrigerant charge, can gradually decrease until a large change has occurred.

It is interesting to look at the cycle time broken down into the on and off portions of the cycle to see how each is affected by a restricted condenser. The data of Table 6.2 is shown in Figure 6.2, below.

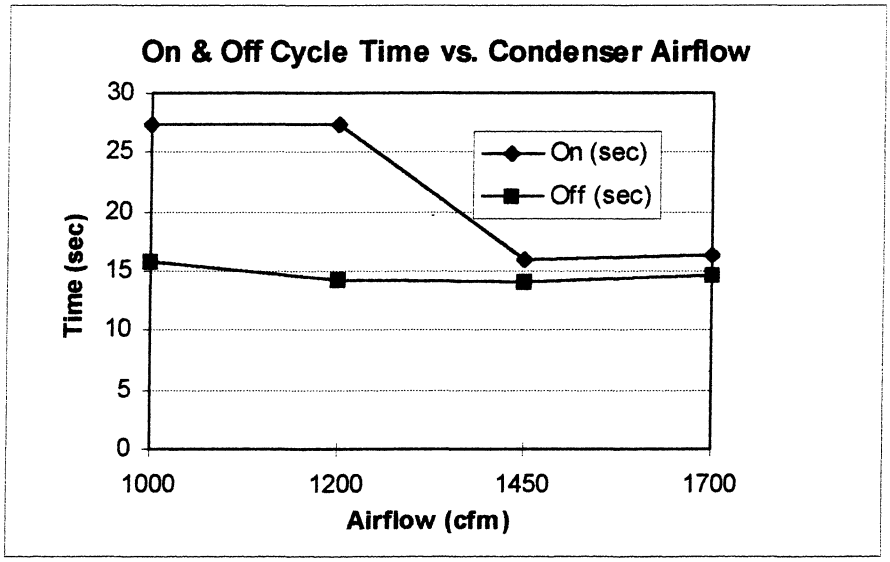

Figure 6.2 Effect of a restricted condenser on the "on" and "off" cycle times.

Figure 6.2 clearly shows that almost all of the change in cycle time occurs during the on part of the cycle. The fact that the off cycle time does not experience a large change could be quite useful. Recall that when charge loss occurs, both the on and off portions of the cycle decrease. Therefore, if a system had both a restricted condenser and low charge, the total cycle time might not change significantly, but the on and off cycle times may change. In other words, to use the cycle time as a tool to detect charge loss, it may be necessary to look at the off and/or on parts of the cycle time as well as the total time.

6.2.2 Effect on T_{ero}.

We have seen the effect that a restricted condenser has on the clutch cycle time, and now we need to determine its effect on T_{ero}. Data was collected from the same five tests of Table 6.1, and the resulting temperatures are given in Table 6.3. Recall that test five did not cycle.

Table 6.3 T_{ero} for a Restricted Condenser.

Test	T_{ero} (°F)	Std Dev
1	31.09	0.62
2	31.74	1.71
3	28.50	0.68
4	29.23	1.15
5	No cycle	---

Figure 6.3 represents the data of Table 6.3 in graphical form below. Figure 6.3 indicates a small drop in T_{ero} of about 2.5 °F at the end of the cycle as the air flow decreases. Like the clutch cycle time, this change occurs between 15% and 30% loss of air flow. Since a restricted condenser does not increase T_{ero}, it would not cause a false positive for refrigerant charge loss. However, the decrease in T_{ero} caused by a reduced air flow is again in contrast to the effect that a loss of refrigerant charge has on T_{ero}. While the effect of a restricted condenser on T_{ero} is small, a few more tests may be necessary in order to determine whether or not it can be ignored when using T_{ero} to detect charge loss.

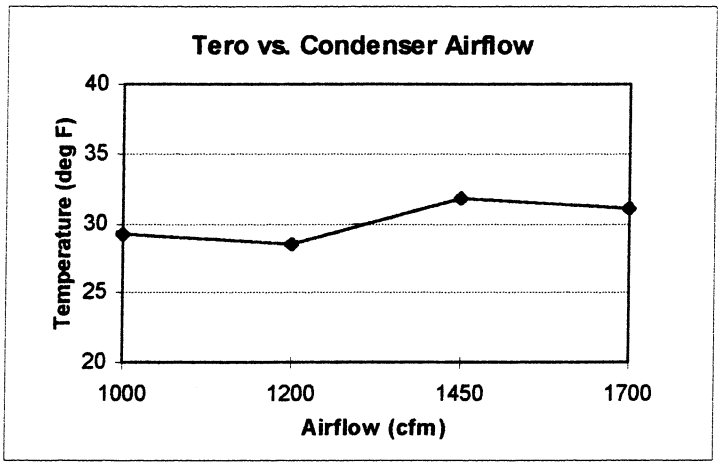

Figure 6.3 T_{ero} vs. Condenser Air Flow.

6.3 Combined Effect of Charge Loss and Condenser Air flow Reduction.

As discussed in the introduction, it is important to see what happens to the system variables being measured when both system faults are occurring at the same time. The same tests of Table 6.1 were conducted again with the refrigerant charge reduced by

20%. Note that test five was not conducted this time since it did not cycle under full charge conditions.

6.3.1 Effect on Clutch Cycle Time.

The test parameters are given in Table 6.4. As in section 6.2.1, once the data had been taken, the off, on , and total cycle times were computed. A comparison of cycle times was made between these low charge tests and the ones of section 6.2.1 with the system at full charge. As before, the resulting on, off, and total cycle times and standard deviations are given in Table 6.5.

Table 6.4 Parameter Values for Restricted Condenser-Low Charge Tests.

Test	Cond. Air Flow (cfm)	Cond. Air Temp (°F)	Evap. Air Temp (°F)	Ref. Charge (lbs)	Comp. Speed
1	1700	100	70	2.35	1950
2	1450	100	70	2.35	1950
3	1200	100	70	2.35	1950
4	1000	100	70	2.35	1950

Table 6.5 Cycle Times for Restricted Condenser-Low Charge Tests.

Test	On (sec)		Off (sec)		Total (sec)	
	Cycle	Std Dev	Cycle	Std Dev	Cycle	Std Dev
1	14.17	0.84	16.95	0.75	31.18	1.43
2	11.74	0.96	14.46	0.54	26.19	1.09
3	14.31	0.30	16.01	0.68	30.32	0.77
4	14.55	0.99	15.89	0.63	30.44	1.14

Figure 6.4 shows the comparison of the "off" cycle times for the different condenser air flow rates. A reduction in air flow causes a slight increase in the off cycle time similar to the small increase for the full charge tests.

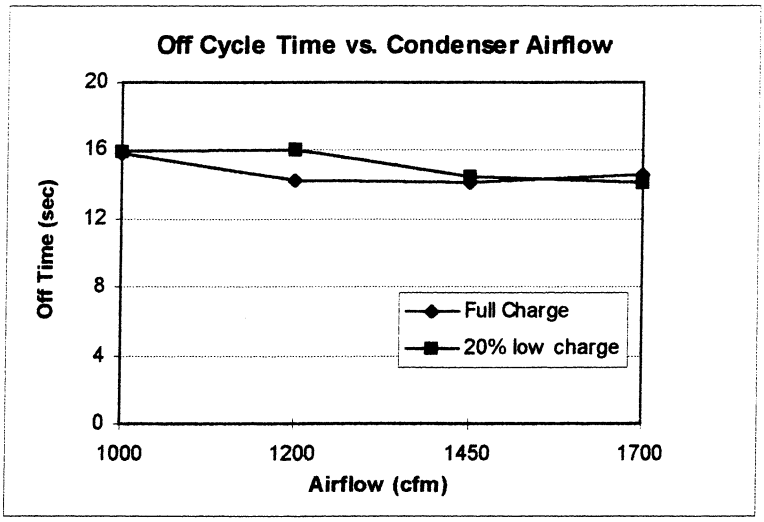

Figure 6.4 Effect of restricted condenser on the "off" cycle times for full and 20% low charge.

Figure 6.5 shows the on cycle times from Table 6.5. The reduction in air flow has very little effect on the "on" cycle time when the charge is 20% low. Since the on time does not increase at low charge as the air flow is reduced, a small gap is maintained between the full and low charge tests.

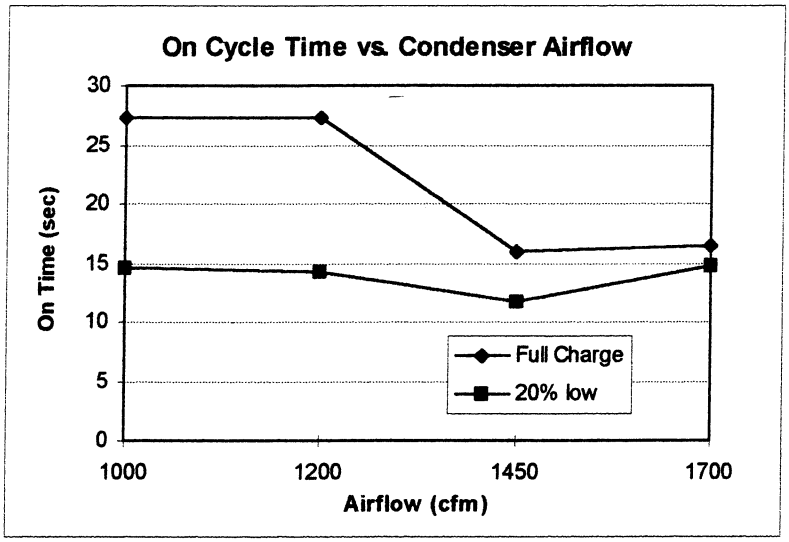

Figure 6.5 A comparison of the "on" cycle times vs. condenser air flow for full and 20% low charge.

Figure 6.6 is a plot of the total cycle time versus condenser air flow for the full and 20% low charge tests. The low charge cycle time increases slightly at low air flow rates due to the slight increase in the off part of the cycle. While the change is not nearly as much as with the full charge, the increase makes it impossible to distinguish between the two curves. The low charge tests at 1000 and 1200 cfm look like the full charge tests at 1450 and 1700 cfm.

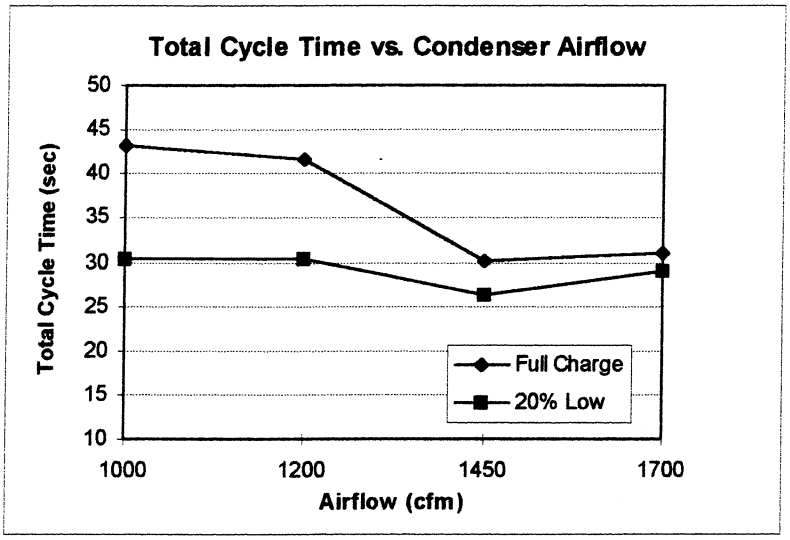

Figure 6.6 Total cycle time vs condenser air flow for full and 20% low charge tests.

6.3.2 Effect on T_{ero}.

In section 6.2.2 we saw what effect a restricted condenser air flow has on a system with a full charge. A restricted condenser caused a small drop in T_{ero}, and this is in contrast to the effect that a low charge has on T_{ero}. It is important to see what happens if both faults occur at the same time in order to see if the effect of each on T_{ero} will cancel each other out. The resulting temperatures from the four tests of Table 6.5 are listed in Table 6.6. The temperature, T_{ero}, is very consistent, and, as usual for T_{ero}, the standard deviations are quite small.

Table 6.6 T_{ero} for a Restricted Condenser-Low Charge.

Test	Low (°F)	Std Dev
1	37.68	0.71
2	37.20	0.64
3	37.50	0.39
4	37.58	0.88

The data from Table 6.6 is plotted below along with the data from Table 6.3 for a fully charged system. The graph clearly shows that T_{ero} is practically a flat line when the system is 20% low on charge, and this is definitely a positive result. If T_{ero} had dropped several degrees at lower air flows for the 20% low charge tests, it might have been indistinguishable from T_{ero} at higher air flow rates. As it turns out, the large gap in T_{ero} between a full charge and low charge is maintained throughout the range of air flows tested.

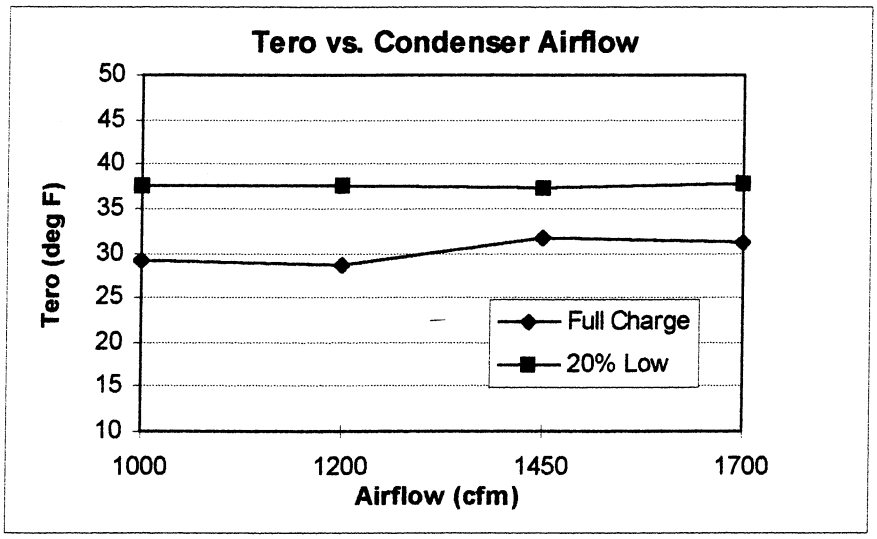

Figure 6.7 T_{ero} vs. condenser air flow for full and 20% low charge.

6.4 Conclusions of Restricted Condenser Tests.

As discussed in the beginning of this chapter, for many vehicles the possibility of getting a condenser fouled with dirt, leaves, and other debris is high enough that it must be taken into consideration. The tests showed that once the condenser air flow was reduced by more than 15%, the clutch cycle time of the system increased significantly

when fully charged. However, when the system is 20% low on charge the cycle time only increases by a small amount after 15% loss of air flow. This slight increase causes a problem for using the cycle time as a tool to detect charge loss. A reduction in charge acts to shorten the cycle time, but at the same time a reduction in air flow increases the cycle time. Thus when looking at the system cycle time the two faults cancel each other out. This is shown in Figure 6.6 of section 6.3.1. A small difference, however, is maintained between the full and low charge tests when only the "on" part of the cycle is considered.

The effect of a restricted condenser on T_{ero} was not as great as for the cycle times. For a fully charged system, T_{ero} decreased slightly after a 15% reduction in the air flow rate; therefore, it will not cause a false positive for charge loss. The restricted condenser caused practically no change in T_{ero} when the system was 20% low in refrigerant charge. Since T_{ero} did not drop during the low charge tests, there is no cancellation effect between the two faults, as was the case for the cycle time. While a restricted condenser is not good for the system, it should not be a roadblock for using T_{ero} to detect refrigerant charge loss.

7. CONCLUSIONS.

7.1 Objective.

As you know by now, the main purpose of this study was to develop an inexpensive and reliable on-line method of detecting refrigerant charge loss from an automotive air conditioning system. The goal is to detect the lowest amount of charge loss possible without running the risk of false positives. The current practice used by mechanics is to measure the off and on portions of the cycle time (for clutch cycling systems) and compare the measured data to predetermined cycle times. If the refrigerant charge is low, the on and off portions of the clutch cycle time should be shorter than expected. However, if you were to look at a mechanic's manual you would see that the range of acceptable cycle times is quite large. This is a good indication that the cycle time is affected by other system and environmental parameters as well. The large range of acceptable cycle times indicates that a large amount of charge must be lost before the cycle time drops low enough for the mechanic to have confidence in the cause of the short cycle times.

7.2 Conclusions.

We started by attempting to detect a 10% loss of charge. The 2^5 design matrix discussed in section 4.2 showed that it would be difficult to detect 10% charge loss using the cycle time. Refrigerant charge did have the largest effect on the cycle time, but a number of other main and interaction effects were quite large. The cycle time data also included a good bit of noise, and this resulted in an equation that was not a very good fit of the original data. Tests were conducted where the evaporator air relative humidity was varied from 20% to 80% with a 20% loss of charge. The humidity had a big impact on the cycle time, and this made it impossible to detect the charge loss without knowing what the humidity was. Since measuring humidity is quite expensive and impractical in such an environment, this presents a problem.

The humidity tests that were conducted at higher evaporator air temperatures, 80 and 85 °F, resulted in the system only cycling at lower values of humidity, and there was a significant difference in the cycle times in this region. If the system is cycling, the humidity must be low, and it is no longer a variable. While this is promising, the method

is restricted to an area where the evaporator air inlet temperature is high and the humidity is low. In some climactic regions these conditions may rarely be seen under normal conditions. With today's on-board computers, the system could be forced into such a region, but tests have shown that the average passenger is uncomfortable under such high temperatures.

We began investigating the possibility of using the refrigerant temperature at the evaporator outlet, T_{ero}, to detect charge loss. At full charge the system is designed to have a high quality at the evaporator outlet; therefore, if the pressure is known, the temperature is known as well. At the end of each cycle, when the clutch disengages, the pressure is 25 psig; therefore the temperature should be around 30.5 °F. If a significant amount of charge is lost the refrigerant is driven into the superheated region at the evaporator outlet. If the refrigerant temperature is well above the saturated temperature at the end of a cycle, significant charge loss must have occurred.

We went back to the same tests that were used to acquire the cycle time data to see how the other system parameters affected T_{ero}. The 2^5 design matrix showed that the refrigerant charge had the largest effect on T_{ero}. There was also very little noise in the data, and the resulting equation fit the data extremely well. However, the temperature difference for the 10% reduction in charge is not great indicating that the low charge tests are just entering the superheated region.

The humidity tests revealed that the evaporator air inlet humidity had basically no effect on T_{ero}. As the humidity was varied, there was no significant change in T_{ero} for a fully charged system. When the system was 20% low on charge T_{ero} increased slowly as the humidity increased, but this is not a concern. The increase only helps widen the gap in T_{ero} between the full and low charge tests. The result is that the humidity does not have to be accounted for when using T_{ero} to detect charge loss. Tests also showed that using T_{ero} was valid over a wide range of evaporator air inlet temperatures.

One concern is that another system fault could trigger a false positive for refrigerant charge loss. One possible fault, especially for off-road and farm machinery, is a partially clogged, restricted, condenser which reduces the air flow. This affects the system by reducing the rate of heat transfer out of the system. Air flow reductions of

more than 15% resulted in greatly increased cycle times for a fully charged system and slightly increased cycle times for 20% low charge. This slight increase when the system is low on charge is not good because it is in contrast to the decrease in cycle time caused by charge loss. If the two system faults occur during the same period of time, they could counteract one another and go undetected. A restricted air flow has no significant impact on T_{ero}. At air flow reductions of more than 15%, T_{ero} drops slightly for a fully charged system, but this is not a problem. The small drop in T_{ero} only increases the gap between the full and low charge tests.

While the cycle time is a free variable, it does not look promising as a tool to detect small amounts of refrigerant charge loss. The fact that a number of other variables also have a significant impact on the clutch cycle time makes it more difficult to detect the charge loss. The impact that humidity has on the cycle time is a concern. The standard deviations of the cycle time can also be quite large making it necessary to average the cycle times over a period of time.

Using T_{ero}, however, would be easy to implement. Simply measure the temperature when the clutch disengages and compare it to the expected value. If the measured value is significantly higher than expected, charge loss has occurred. The expected value may increase slightly at higher evaporator air inlet temperatures, but this can be easily accounted for. The fact that the other system parameters do not need to be accounted for in order to use T_{ero} makes it a very simple method to implement. Our tests show that this method could easily detect 20% charge loss, and this is a big improvement over the methods that are currently being used.

7.3 Future Work.

Although the tests were conducted using an actual air conditioning system, verifying the results for the evaporator outlet refrigerant temperature method on one or more actual vehicles would strengthen the idea that the method is general to all orifice tube, fixed-displacement compressor systems. A mobile air conditioning system model is currently being developed on this same project. Once it is completed and validated, some tests should be performed on it to make sure that our laboratory test results agree with the model.

Two other types of mobile air conditioning systems are commonly found in today's market: 1) systems using thermal expansion valves (TXV's) with fixed-displacement compressors, and 2) systems with orifice tubes and variable displacement compressors. The TXV systems are designed to maintain a small amount of superheat at the outlet of the evaporator; therefore, our proposed method would not work on this type of system. The variable displacement compressors are designed to maintain a specified pressure at the evaporator outlet in order to maintain a high quality at the evaporator outlet. With the pressure held constant, if charge loss occurs, the refrigerant should become superheated, increasing T_{ero}. If this is the case, our method would work with this type of system as well. However, laboratory tests on this type of system would need to be conducted before any conclusions could be drawn.

LIST OF REFERENCES

[1] C.A. Amann, "The Passenger Car and the Greenhouse Effect," SAE Transactions, Volume 99, Section 6, 1990, pp. 1646-1665.

[2] "A/C Refrigerant Systems Reference Manual," Confidential.

[3] Hans Magg, "Elastomers for Automotive Air Conditioning Hoses," SAE Technical Paper Series, paper number 900575, 1990.

[4] H. Inatsu, et al, "Development of Refrigerant Monitoring System for Automotive Air Conditioning System," SAE Transactions, Volume 101, pp. 29-37, 1992.

[5] David J. Bateman, "Performance Comparison of HFC-134a and CFC-12 in an automotive Air Conditioning System," SAE Technical Paper Series, paper number 890305, 1989.

[6] C. Piao, H. Sato, and K. Watanabe, "Thermodynamic Charts, Tables, and Equations for Refrigerant HFC-134a," ASHRAE Transactions, Volume 97, Part 2, 1991, pp. 268-284.

[7] J. J. Grebner, R. R. Crawford, "Measurement of Pressure-Temperature-Concentration Relations for Mixtures of R-12/Mineral Oil and R-134a Synthetic Oil," ASHRAE Transactions, pp. 387-396.

[8] P.G. Weston, "Design and Construction of a Mobile Air Conditioning System Test Facility for Transiient Studies," M.S. Thesis, University of Illinois, 1996.

[9] J. R. Rubio-Quero, "A Facility for Transient Testing of Mobile Air Conditioning Systems," M.S. Thesis, University of Illinois, 1995.

[10] C. D. Collins, " Experimental Study of Mobile Air Conditioning System Transient Behavior," M.S. Thesis, University of Illinois, 1996.

[11] M. Whitchurch, "Humidity Effects in Mobile Air-Conditioning Systems," M.S. Thesis, University of Illinois, 1997.

[12] E. Wandell, "Experimental Investigation of Mobile Air Conditioning System Control for Improved Compressor Reliability," M.S. Thesis, University of Illinois, 1997.

[13] OMEGA, The Temperature Handbook. Omega Engineering, Inc., Volume 28, 1992, pp. Z17-18.

[14] R.E. DeVor, T. Chang, and J.W. Sutherland, Statistical Quality Design and

Control: Contemprary Concepts and Methods. Macmillan: New York, 1992.

[15] G. E. P. Box, W. G. Hunter, and J. S. Hunter, Statistics for Experimenters: John Wiley & Sons, 1978.

[16] W. F. Stoecker, Design of Thermal Systems, Third Edition, McGraw-Hill: New York, 1989.

[17] H. Kawamoto, et al, "Comfort Evaluation of Heating and Air Conditioning Systems," SAE Special Publications: SP-668, Published by SAE, Warrendale, PA, 1986, p. 61-67.

[18] S. A. Klein and F. L. Alvarado, "Engineering Equation Solver," Version 4.305W, F-Chart Software, Middleton, WI, 1992.

[19] L. M. Schlager, M. B. Pate, and A. E. Bergles, "Oil Quantity Measurements in Smooth and Micro-fin Tubes During Evaporation and Condensation of Refrigerant-Oil Mixtures," ASHRAE Transactions: Vol. 96 Pt. 2, 1990, pp. 465-469.

APPENDIX A. DATA REDUCTION

As was discussed earlier, there are two data acquisition systems currently being used to acquire data in the lab. For the SOMAT 2500 system that I added, see section 2.5.2, a data acquisition program had to be developed. Since the SOMAT samples at a minimum of 100 Hz, spreadsheet programs such as Excel are not capable of handling that many rows of data. I chose to use Matlab in order to reduce and analyze the data. Matlab can handle larger data sets, and the multi-channel data fits nicely into the matrix format used by Matlab. Using "*.m" files, like the one below, can also save time. By typing only the file name, Matlab reads in the raw data, converts it to desired parameters, analyzes and reduces the data, and makes plots of requested data. The program below was written to reduce the data acquired by the TCE file named "cycle" on the lab computer. The channels that are read into Matlab are the evaporator outlet refrigerant temperature and pressure, the voltage signal being sent to the compressor clutch, time, and the signal being sent to the HP acquisition system.

```
%************************************************************
%Cleveland E. Johnston
%07/25/96
%University of Illinois at Urbana-Champaign
%ACRC Project 51 - Mobile A/C System

% The purpose of this Matlab program is to reduce the data acquired
% from the SOMAT 2500 DAQ. It's main function is to compute the
% clutch cycle times and record the refrigerant temperature at the
% evaporator outlet at the end of each "on" cycle (when the clutch is
% disengaged.
%************************************************************

clear

%************************************************************
% This first section reads in the raw data (note: the data must be
% converted from a .sif (SOMAT) file to a .txt file. This is done using
% EASE. The channels are as follows:
% 1.) The voltage being sent to the clutch
% 2.) The signal sent to the HP DAQ system
% 3.) The temperature at the evaporator outlet
```

```
% 4.) The pressure at the evaporator outlet
% 5.) The time
%*************************************************************

fid = fopen('d:\research\Tero_2\test9c.txt');
[B,count] = fscanf(fid,'%f %f %f %f %f',[5,inf]);

B = B';
count = count/5;
%B(1000, 3)
B(:,3) = B(:,3)/1000;        %****Converts temp. from Volts to mV****

%*************************************************************
% This section converts the pressure signal to psig and then filters the
% signal.
%*************************************************************

m_Pero = 20.038;
Vo_Pero = .097977;
P_atm = 14.7;
B(:,4) = m_Pero*(B(:,4)-Vo_Pero);
B0 = B(:,4);
b = ones(1:10)/10;
pressure = filtfilt(b,1,B(:,4));
B(:,4) = pressure;

%*************************************************************
% This section converts the temperature signal from mV to degrees
% Fahrenheit.
%*************************************************************

a0 = 0.10086091;
a1 = 25727.94369;
a2 = -767345.8295;
a3 = 78025595.81;
a4 = -9247486589;
a5 = 6.97688*10^11;
a6 = -2.66192*10^13;
a7 = 3.94078*10^14;

Tc = a0+a1*B(:,3)+a2*B(:,3).^2+a3*B(:,3).^3+a4*B(:,3).^4+a5*B(:,3).^5+
     a6*B(:,3).^6+a7*B(:,3).^7;
Tf = (9/5)*Tc+32;
B(:,3) = Tf;
```

```
%************************************************************
% This section converts the clutch signal to a smooth square signal for
% easier viewing purposes.
%************************************************************

for i = 1:count
   z = 0.001;
   if B(i,1) > z
         C(i,1) = 1;
         else C(i,1) = 0;
   end
end

%************************************************************
% The next section is the main body of the program.  The n* and m*
% constants help keep track of the beginning and end of each "on" and
% "off" part of the cycle.  When the clutch signal goes to 0 the program
% records the length of the "on" part of the cycle time and Tero.  When
% the clutch signal goes from 0 to 1, the program records the "off" part
% of the cycle time.
%************************************************************

n1 = 1;
n2 = 1;
n3 = 1;
m1 = 0;
m2 = 0;
m3 = 0;

z = 6;
switch = 0;

for j = 11:count-11
 if j > switch + 10
  if B(j+1) < z & B(j) > z
     m1 = m1+1;
        n1 = j;
     switch = j;
        Cycle(m1,1) = B(n1,5) - B(n2,5);
     Tlow(m1) = B(n1,3);
  elseif B(j+1) > z & B(j) < z
        m2 = m2+1;
        n2 = j;
     switch = j;
        Cycle(m2,2) = B(n2,5) - B(n1,5);
```

```
      Thigh(m2) = B(n2,3);
    end
  end
    if mean(B(j-10:j+10,4))<29&j>n3+500
        m3 = m3+1;
        n3 = j;
        Ptime(m3,1) = B(n3,5) - B(n2,5);
    end
end

%*************************************************************
% TC sums the "on" and "off" portions of each cycle found above in
% in order to get the overall cycle times.
%*************************************************************

TC = sum(Cycle')';

%*************************************************************
% y, m, and l are used to find the smallest matrix in order to keep from
% exceeding the limits of the matrix.
%*************************************************************

y = min([m1 m2]);
m = max([m1 m2]);
l = min([m m3]);

%*************************************************************
% This loop takes the high and low refrigerant temperatures measured
% at the evaporator outlet at the beginning and end of each cycle,
% respectively, and puts them into one matrix for simplicity.
%*************************************************************

for i = 1:y
   Temp(i,1) = Thigh(i);
   Temp(i,2) = Tlow(i);
   Temp(i,3) = Thigh(i)-Tlow(i);
end

%*************************************************************
% This adds TC and Ptime to the matrix that already contains the "on"
% and "off" cycle times for simplicity.  Then the first and last cycles are
% removed to ensure that only compete cycles are used to compute the
% mean and standard deviations.
%*************************************************************
```

```
for i = 1:l
   Cycle(i,3) = TC(i);
   Cycle(i,4) = Ptime(i);
end

[n,m] = size(Cycle);
Cycle(1,:) = [];
Cycle(n,:) = [];

%*************************************************************
% This section computes the mean and standard deviations and sends
% these along with the original cycle and temp data to the screen.
%*************************************************************

Cycle
avg = mean(Cycle2)
stddev = std(Cycle2)

Temp
avg = mean(Temp)
stdev = std(Temp)

%*************************************************************
% This section sets up the plot window(s) including titles, labels, axes
% limits, etc, and then it plots the requested data vs. time.  This section is
% slightly modified for each test.
%*************************************************************

figure
subplot(3,1,1)
hold

%****Plots T_ero vs. time****
plot(B(:,5),B(:,3),'w');

%****Plots Evap Outlet Pressure vs. time****
plot(B(:,5),B(:,4)-5,'w');

%****Plots the clutch signal vs. time****
plot(B(:,5),C(:,1)*5+3,'w');

hold off

%****Controls which section of the plot area is shown****
axis([40 110 0 50]);
```

```
%****Adds labels, gridlines, and other text to the plot window****
title('20% Charge Loss');
xlabel('Time (sec)');
grid

end
```

APPENDIX B. DISCUSSION OF 2^K FACTORIAL EXPERIMENTS.

In this section, I will attempt to briefly summarize the basic approach and analysis of a 2^k factorial design matrix. A much more detailed discussion of 2^k designs, as well as fractional factorial designs can be found in [14] and [15]. To facilitate the discussion I will present, discuss, and analyze a specific example, the pressure drop across an orifice tube. For many applications two-level, 2^k, factorial design matrices are a very useful tool for a test engineer because they exhibit many of the qualities that make up a good design of experiments. Fore instance, they can include qualitative factors. For example, one of the test parameters could be the orifice tube material. The two parameter levels could be plastic and steel, and the effect of a particular material on the outlet pressure could be analyzed.

A set of tests will be carried out to study how the pressure drop across an orifice tube is affected by the diameter of the tube and the flow rate of the fluid, in this case R134a refrigerant. Other parameters, such as the length of the orifice tube, could possibly affect the pressure drop as well, but for this example it is assumed that all other parameters are either constant or have no effect on the pressure drop. Currently an orifice tube of 0.06 inches is being used at a flow rate of 250 lbm/hr, and we want to see what happens to the pressure drop if the orifice tube is decreased to 0.05 inches and/or the flow rate to 200 lbm/hr. Since there are only two parameters, this is a 2^2 design matrix. The two levels for each factor are shown in Table B.1, and the resulting four different possible combinations of the two parameters are shown in Table B.2.

Table B.1 Parameter Values for Pressure Drop Tests.

Tag	Parameter		High (+)	Low (-)
1	Tube diameter	[inches]	0.06	0.05
2	Flow rate	[lbm/hr]	250	200

Table B.2 Test Matrix for Pressure Drop Experiment.

	Parameter	
Test	1	2
1	-	-
2	+	-
3	-	+
4	+	+

Once the system reaches steady-state, the pressure upstream and downstream of the orifice tube is taken every second for a period of one minute. After averaging the 60 data points for each of the four tests, the resulting data is shown in Table B.3.

Table B.3 Results of Pressure Drop Tests.

	Parameter		Pressure	Std Dev
Test	1	2	Drop (psi)	(psi)
1	-	-	113	3.3
2	+	-	105	1.9
3	-	+	128	4.2
4	+	+	110	3.1

Figure B.1 shows the effect that the orifice tube diameter has on the pressure drop while the flow rate is held constant. For both flow rates the larger diameter causes a decrease in the pressure drop, but the drop is much larger when the flow rate is at its higher value of 250 lbm/hr. Thus, the effect that the tube diameter has on the pressure drop is dependent upon the value of the flow rate, and this dependence, or interaction, must be considered.

When the orifice tube diameter is held constant, an increase in flow rate causes an increase in the pressure drop, shown in Figure B.2. Figure B.2 also shows the interaction between the flow rate and tube diameter. The increase in pressure drop is greater for the small diameter (15 psi) than for the large diameter (5 psi). These parameter interactions add a lot of complexity to the problem

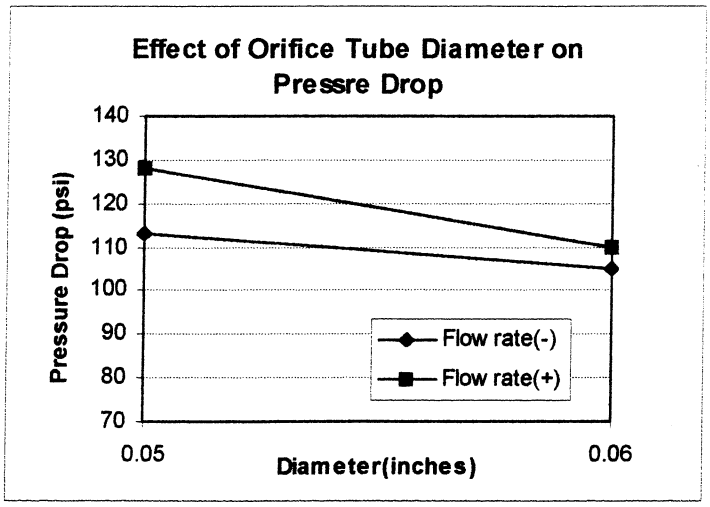

Figure B.1 Orifice tube diameter vs. Pressure drop with constant flow rates.

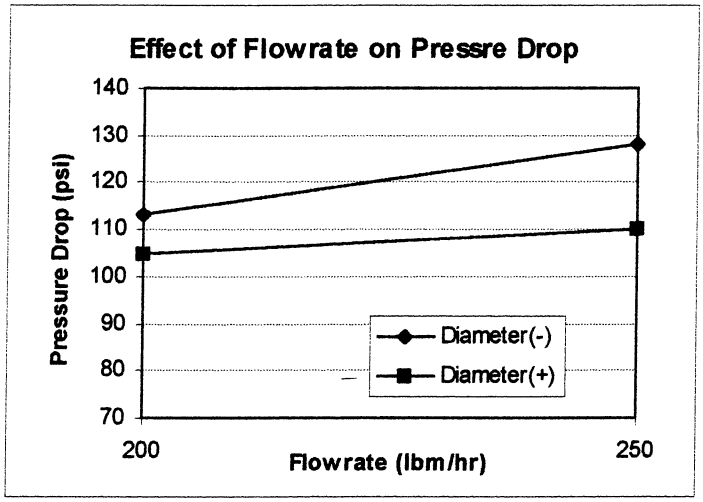

Figure B.2 Flow rate vs. Pressure drop with constant orifice tube diameters.

To calculate the overall main effect of orifice tube diameter on the pressure drop, we must take the average of the pressure drops over the two values of flow rate:

$E_1 = (^2/_N)*[(Y_2-Y_1) + (Y_4-Y_3)]$

$E_1 = (^1/_2)*[(105 - 113) + (110 - 128)]$

$E_1 = -13$

E_1 represents the average change in pressure drop due to an increase from 0.05 to 0.06 inches for the orifice tube. The main effect for the flow rate is calculated in a similar manner:

$E_2 = (^2/_N)*[(Y_3-Y_1) + (Y_4-Y_2)]$

$E_2 = (^1/_2)*[(128 - 113) + (110 - 105)]$

$E_2 = 10$

The computations of E_1 and E_2 are relatively easy to follow, especially from Figures B.1 and B.2, but the interaction effect may be a little harder to visualize. We have already shown that the flow rate effect is 5 for the larger orifice tube and 15 for the smaller tube, and that the main effect for flow rate is the average of these two values. The dependency of flow rate on the tube size is found by taking the difference between the two values and then dividing by two:

$$E_{12} = \frac{[(110-105)-(128-113)]}{2}$$

$$E_{12} = \frac{5-15}{2}$$

$E_{12} = -5$

It is not very difficult to see and interpret the main and interaction effect for the two parameter case of this example, but for a higher number of parameters, an easier mathematical method is needed. We will refer to Table B.4 in order to facilitate the mathematical interpretation.

Table B.4 Calculation of Effects.

Test	x1	x2	Y (psi)
1	-1	-1	113
2	+1	-1	105
3	-1	+1	128
4	+1	+1	110

To determine the main effect of orifice tube diameter, we can simply multiply the Y value for each test by the ±1 found in the x1 column and then divide the sum by N/2, where N is the total number of tests.

x1		Y
-1	x	113
+1	x	105
-1	x	128
+1	x	110
Sum	=	-26
Sum/2	=	-26/2
E_1	=	-13

The resulting main effect for the orifice tube diameter is -13, which agrees with the graphical analysis. The main effect for the flow rate is calculated in the same manner.

x2		Y
-1	x	113
-1	x	105
+1	x	128
+1	x	110
Sum	=	20
Sum/2	=	20/2
E_2	=	10

Once again, the mathematical approach agrees with the graphical method previously described. To calculate the interaction effect, it is necessary to multiply Y by both the ±1 value of column x1 and x2.

x1		x2		Y		
-1	x	-1	x	113		113
+1	x	-1	x	105	=	-105
-1	x	+1	x	128		-128
+1	x	+1	x	110		110
				Sum	=	-10
				Sum/2	=	-10/2
				E_{12}	=	-5

As expected, the interaction effect, E_{12}, is equal to -5, as was found earlier. This same approach can be taken for higher degrees of interactions, if the design includes more than two variables.

Now that the main and interaction effects have been calculated, an equation for the pressure drop can be developed.

$PD = b_0 + b_1*x1 + b_2*x2 + b_{12}*x1*x2$

where,

PD = pressure drop.

b_0 = average of all tests.

$b_i = E_i/2$.

The calculated effects, E_i, measure the change in Y for a two unit change in x (from -1 to +1). The mathematical model is based on a one unit change in x; so, the effects must be divided by 2.

$b_0 = 114$

$b_1 = E_1/2 = -13/2 = -6.5$

$b_2 = E_2/2 = 10/2 = 5.0$

$b_{12} = E_{12}/2 = -5/2 = -2.5$

The resulting equation is:

$PD = 114 - 6.5*x1 + 5.0*x2 - 2.5*x1*x2$

To use the equation for the pressure drop, the two measured variables must be scaled to a value between -1 and +1. For instance, if you wanted to estimate the pressure drop for the case of a 0.54 inch orifice tube and a 240 lbm/hr flow rate, the following values would need to be calculated:

$$\frac{250-200}{1-(-1)} = \frac{240-200}{x1-(-1)}$$

$$\frac{50}{2} = \frac{40}{x1+1}$$

$x1 = 0.6$ and,

$$\frac{0.06-0.05}{1-(-1)} = \frac{0.054-0.05}{x2-(-1)}$$

$$\frac{0.01}{2} = \frac{0.004}{x2+1}$$

$x2 = -0.2$

Therefore, the estimate of the pressure drop is,

PD = 114 - 6.5*(0.6) + 5.0*(-0.2) -2.5*(0.6)*(-0.2)

PD = 114 - 3.9 - 1.0 + 0.3

PD = 109.4 psi

As you have probably already noticed, the resulting equation assumes a linear fit between the low and high value of each parameter. For instance it assumes that the pressure drop changes linearly with a change in the flow rate, as is implied in Figure B.2. This may not be the case, however, and one must be careful when making such an assumption. Once the equation has been formed, it is wise to check for nonlinearity by conducting a few tests at intermediate parameter values. Another important note is that the resulting equation should only be used in the region bounded by the low and high values for each parameter. For instance, if one wanted to see what value for the pressure drop would result from an orifice tube of 0.05 inches and a flow rate of 275 lbm/hr, the above equation should not be used. Due to the possibility of nonlinearities, as just discussed. If the equation is used for extrapolation of a parameter, the resulting pressure drop should be used with caution.

Although the two parameter case above is quite simple, the methods can be easily expanded to include more parameters. Once the equation has been formed, the validity of the model should be checked and the model modified as necessary. For more details on model validation, refer to section 4.2 of this thesis or [14] and [15]. 2^k design matrices work well for a small number of variables, but as the number of parameters increase, the number of required tests increases rapidly:

# of parameters	# of tests
2	4
3	8
4	16
5	32
7	128
10	1024

For many systems with a large number of parameters, it would be impractical to perform so many tests. In such a case, either fractional factorial design matrices or some other smaller set of tests would need to be conducted.